regions of parent-specific CpG methylation are established after fertilization and are not associated with dimethyl Lys9 H3.

(3) Consequences of deletion of the IC are the same as those of CpG methylation and H3 dimethylation of the IC.

(4) ICs contain promoters of noncoding transcripts in the case of DMR-*LIT1* and the *Igf2r* imprinting control element, and of a transcript encoding *SNRPN* and *SNURF* proteins in the case of the PWS-IC; in all three regions, effects of antisense transcription cannot account for all observed imprinting phenomena.

The coincidence between germ-line-established maternal-specific CpG methylation and the presence of dimethyl Lys9 H3 at all three ICs is striking, and raises the possibility that there may be a causal relationship between establishment of these epigenetic marks in the germ-line. These epigenetic marks appear to inactivate the ICs, rather than to modulate the function of the ICs; for all three ICs, the effect of an IC deletion is the same as the effect of a maternal CpG-methylated and H3 Lys9-methylated IC.

How does an unmethylated IC act to influence gene expression bidirectionally over distances of up to 1 Mb? Several possibilities have been raised in the literature.

(1) Unmethylated ICs act as enhancer blockers that protect imprinted genes from effects of distant enhancers. This hypothesis requires that each imprinted gene regulated by an IC has an enhancer on the other side of the IC. Mancini-DiNardo et al. [2003] showed that an unmethylated DMR-*Lit1* does not act as enhancer blocker, which blocks transcription only when placed between enhancer and promoter, but rather acts as silencer, which blocks transcription even when not placed between enhancer and promoter. This hypothesis is also clearly not applicable to the PWS/AS region, where most imprinted genes are paternally-active, in cis with an unmethylated PWS-IC.

(2) Noncoding RNAs act in cis to regulate gene expression. Sleutels et al. [2002] showed that, in the mouse *Igf2r* imprinted cluster, truncation of the noncoding *Air* RNA that is transcribed from its promoter in the IC causes loss of imprinting for all genes in the cluster. However, in the PWS/AS region, a deletion extending from *Snrpn* intron 1 to *Ube3a* intron 1 removes almost all of the paternally-expressed region downstream from the PWS-IC, but paternal deletion of this region has no effect on imprinted expression of *Ndn* [Tsai et al., 1999].

(3) Unmethylated ICs act as silencers and establish a repressive chromatin structure bidirectionally over long distances, until boundary elements are reached that prevent further spread of the repressive chromatin structure. More generally, an unmethylated IC on a paternal chromosome acts to establish a modified chromatin structure different from that on the maternal chromosome which has a methylated, nonfunctional IC. According to this hypothesis, the transcriptional activity of individual genes is a function of the interaction of promoters/enhancers with modified chromatin structure. For some genes, a paternal-specific chromatin structure may be activating; for other genes, the same chromatin structure may be repressive. At this point, the only evidence for contiguous spread of a modified chromatin state through an imprinted region comes from the mouse *Kip2/Lit1* domain in placenta, which shows paternal-specific association with dimethyl Lys9 H3 and trimethyl Lys27 H3 in promoters, genes, and intergenic regions [Umlauf et al., 2004]; this contiguous region of altered chromatin structure on the paternal chromosome is not present in 9.5 day p.c. embryos.

Whether the apparent similarities of structural organization and epigenetic marking of the IC between these imprinted regions actually reflect common mechanisms by which ICs affect gene expression bidirectionally over long distances will only become clear as the mechanisms of gene regulation in the PWS/AS region, the *KIP2/LIT1* domain of the BWS region, and the mouse *Igf2r* region are elucidated. Current data for the *Igf2r* region are compatible with a mechanism of RNA-mediated regulation in cis similar to *Xist*-mediated X chromosome inactivation. However, there is no published evidence as yet for association of the noncoding *Air* RNA with this region, and the

roles (if any) of noncoding RNAs in imprinting of the PWS/AS and *KIP2/LIT1* regions remain to be explored.

The concept of ICs as sites from which modified chromatin structures are propagated bidirectionally and maintained is attractive as a general explanation for the epigenetic phenomena observed in these three regions. Future research on parent-specific association of noncoding RNAs, histone variants, modified histones, and nonhistone chromosomal proteins with these regions promises to shed light on the complexities of these imprinted clusters and their roles in human disease.

REFERENCES

Albrecht U, Sutcliffe JS, Cattanach BM, Beechey CV, Armstrong D, Eichele G, Beaudet AL. 1997. Imprinted expression of the murine Angelman syndrome gene, *Ube3a*, in hippocampal and Purkinje neurons. Nat Genet 17:75–78.

Bielinska B, Blaydes SM, Buiting K, Yang T, Krajewska-Walasek M, Horsthemke B, Brannan CI. 2000. De novo deletions of *SNRPN* exon 1 in early human and mouse embryos result in a paternal to maternal imprint switch. Nat Genet 25:74–78.

Buiting K, Saitoh S, Gross S, Dittrich B, Schwartz S, Nicholls RD, Horsthemke B. 1995. Inherited microdeletions in the Angelman and Prader–Willi syndromes define an imprinting center on human chromosome 15. Nat Genet 9:395–400.

Buiting K, Lich C, Cottrell S, Barnicoat A, Horsthemke B. 1999. A 5-kb imprinting center deletion in a family with Angelman syndrome reduces the shortest region of deletion overlap to 880 bp. Hum Genet 105:665–666.

Chung W-Y, Yuan L, Feng L, Hensle T, Tycko B. 1996. Chromosome 11p15.5 regional imprinting: Comparative analysis of *KIP2* and *H19* in human tissues and Wilms' tumors. Hum Mol Genet 8:1101–1108.

Delaval K, Feil R. 2004. Epigenetic regulation of mammalian genomic imprinting. Curr Opin Genet Dev 14:188–195.

Diaz-Meyer N, Day CD, Khatod K, Maher E, Cooper W, Reik W, Junien C, Graham G, Algar E, Der Kaloustian VM, Higgins MJ. 2003. Silencing of *CDKN1C* ($p57^{KIP2}$) is associated with hypomethylation at *KvDMR1* in Beckwith–Wiedemann syndrome. J Med Genet 40:797–801.

Driscoll DJ, Waters MF, Williams CA, Zori RT, Glenn CC, Avidano KM, Nicholls RD. 1992. A DNA methylation imprint, determined by the sex of the parent, distinguishes the Angelman and Prader–Willi syndromes. Genomics 13:917–924.

El-Maarri O, Buiting K, Peery E, Kroise P, Balaban B, Wagner K, Urman B, Heyd J, Lich C, Brannan C, Walter J, Horsthemke B. 2001. Methylation imprints on human chromosome 15 are established during or after fertilization. Nat Genet 27:341–344.

Fitzpatrick GV, Soloway PD, Higgins MJ. 2002. Regional loss of imprinting and growth deficiency in mice with a targeted deletion of *KvDMR1*. Nat Genet 32:426–431.

Fournier C, Goto Y, Ballestar E, Delaval K, Hever AM, Esteller M, Feil R. 2002. Allele-specific histone lysine methylation marks regulatory regions at imprinted mouse genes. EMBO J 21:6560–6570.

Fulmer-Smentek S, Francke U. 2001. Association of acetylated histones with paternally-expressed genes in the Prader–Willi deletion region. Hum Mol Genet 15: 645–652.

Geuns E, De Rycke M, Van Steirteghem A, Liebaers I. 2003. Methylation imprints of the imprint control region of the *SNRPN* gene in human gametes and preimplantation embryos. Hum Mol Genet 12:2873–2879.

Glenn CC, Saitoh S, Jong MTC, Filbrandt MM, Surti U, Driscoll DJ, Nicholls RD. 1996. Gene structure, DNA methylation, and imprinted expression of the human *SNRPN* gene. Am J Hum Genet 58:335–346.

Hatada I, Mukai T. 1995. Genomic imprinting of $p57^{KIP2}$, a cyclin-dependent kinase inhibitor, in mouse. Nat Genet 11:204–206.

Hatada I, Ohashi H, Fukushima Y, Kaneko Y, Inoue M, Komoto Y, Okada A, Ohishi S, Nabetani A, Morisaki H, Nakayama M, Niikawa N, Mukai T. 1996. An imprinted gene $p57^{KIP2}$ is mutated in Beckwith–Wiedemann syndrome. Nat Genet 14:171–173.

Higashimoto K, Urano T, Sugiura K, Yatsuki H, Joh K, Zhao W, Iwakawa M, Ohashi H, Oshimura M, Niikawa N, Mukai T, Soejima H. 2003. Loss of CpG methylation is strongly correlated with loss of histone H3 lysine 9 methylation at DMR-*LIT1* in patients with Beckwith–Wiedemann syndrome. Am J Hum Genet 73:948–956.

Horike S, Mitsuya K, Meguro M, Kotobuki N, Kashiwagi A, Notsu T, Schulz TC, Shirayoshi Y, Oshimura M. 2000. Targeted disruption of the human *LIT1* locus defines a putative imprinting control element playing an essential role in Beckwith–Wiedemann syndrome. Hum Mol Genet 9:2075–2083.

Jackson JP, Lindroth AM, Cao X, Jacobsen SE. 2002. Control of CpNpG DNA methylation by the KRYPTONITE histone H3 methyltransferase. Nature 416:556–560.

Jenuwein T, Allis CD. 2001. Translating the histone code. Science 293:1074–1080.

Kishino T, Lalande M, Wagstaff J. 1997. *UBE3A/E6-AP* mutations cause Angelman syndrome. Nat Genet 15: 70–73.

Lau JC, Hanel ML, Wevrick R. 2004. Tissue-specific and imprinted genetic modificationsof the human *NDN* gene. Nucl Acids Res 24:3376–3382.

Lee MP, DeBaun M, Mitsuya K, Galonek HL, Brandenburg S, Oshimura M, Feinberg A. 1999. Loss of imprinting of a paternally expressed transcript, with antisense orientation to *KvLQT1*, occurs frequently in Beckwith–Wiedemann syndrome and is independent of insulin-like growth factor II imprinting. Proc Natl Acad Sci USA 96:5203–5208.

Lehnertz B, Ueda Y, Derijck AA, Braunschweig U, Perez-Burgos L, Kubicek S, Chen T, Li E, Jenuwein T, Peters AH. 2003. Suv39h-mediated histone H3 lysine 9 methylation directs DNA methylation to major satellite repeats at pericentric heterochromatin. Curr Biol 15:1192–1200.

Lewis A, Murrell A. 2004. Genomic imprinting: CTCF protects the boundaries. Curr Biol 14:R284–286.

Lewis A, Mitsuya K, Umlauf D, Smith P, Dean W, Walter J, Higgins M, Feil R, Reik W. 2004. Imprinting on distal

chromosome 7 in the placenta involves repressive histone methylation independent of DNA methylation. Nat Genet 36:1291–1295.

Lossie AC, Whitney MM, Amidon D, Dong HJ, Chen P, Theriaque D, Hutson A, Nicholls RD, Zori RT, Williams CA, Driscoll DJ. 2001. Distinct phenotypes distinguish the molecular classes of Angelman syndrome. J Med Genet 38:834–845.

Mancini-DiNardo D, Steele SJS, Ingram RS, Tilghman S. 2003. A differentially methylated region within the gene *Kcnq1* functions as an imprinted promoter and silencer. Hum Mol Genet 12:283–294.

Matsuura T, Sutcliffe JS, Fang P, Galjaard R-J, Jiang Y, Benton CS, Rommens JM, Beaudet AL. 1997. De novo truncating mutations in E6-AP ubiquitin-protein ligase gene (*UBE3A*) in Angelman syndrome. Nat Genet 15: 74–77.

Meguro M, Kashiwagi A, Mitsuya K, Nakao M, Kondo I, Saitoh S, Oshimura M. 2001. A novel maternally-expressed gene, *ATP10C*, encodes a putative amino-phospholipid translocase associated with Angelman syndrome. Nat Genet 28:19–20.

Nicholls RD, Knepper JL. 2001. Genome organization, function, and imprinting in Prader–Willi and Angelman syndromes. Annu Rev Genom Hum Genet 2:153–175.

Niemitz E, DeBaun M, Fallon J, Murakami K, Kugoh H, Oshimura M, Feinberg A. 2004. Microdeletion of *LIT1* in familial Beckwith–Wiedemann syndrome. Am J Hum Genet 75:844–849.

Ohta T, Gray TA, Rogan PK, Buiting K, Gabriel JM, Saitoh S, Muralidhar B, Bielinska B, Krajewska-Walasek M, Driscoll DJ, Horsthemke B, Butler MG, Nicholls RD. 1999. Imprinting-mutation mechanisms in Prader–Willi syndrome. Am J Hum Genet 64:397–413.

Riesewijk A, Schepens M, Welch T, van den Berg-Loonen E, Ropers H, Kalscheuer V. 1996. Maternal-specific methylation of the human *IGF2R* gene is not accompanied by allele-specific transcription. Genomics 31:158–166.

Runte M, Huttenhofer A, Gross S, Kiefmann M, Horsthemke B, Buiting K. 2001. The IC-*SNURF-SNRPN* transcript serves as a host for multiple small nucleolar RNA species and as an antisense RNA for *UBE3A*. Hum Mol Genet 10:2687–2700.

Saitoh S, Wada T. 2000. Parent-of-origin specific histone acetylation and reactivation of a key imprinted gene locus in Prader–Willi syndrome. Am J Hum Genet 66:1958–1962.

Schweizer J, Zynger D, Francke U. 1999. In vivo nuclease hypersensitivity studies reveal multiple sites of parental origin-dependent differential chromatin conformation in the 150 kb *SNRPN* transcription unit. Hum Mol Genet 8:555–566.

Shemer R, Birger Y, Riggs A, Razin A. 1997. Structure of the mouse *Snrpn* gene and establishment of its parental-specific methylation pattern. Proc Natl Acad Sci USA 94:10267–10272.

Sleutels F, Zwart R, Barlow DP. 2002. The non-coding *Air* RNA is required for silencing autosomal imprinted genes. Nature 415:810–813.

Tachibana M, Sugimoto K, Fukushima T, Shinkai Y. 2001. SET-domain containing protein, G9a, is a novel lysine-preferring histone methyltransferase with hyperactivity and specific selectivity to lysines 9 and 27 of histone H3. J Biol Chem 27:25309–25317.

Tachibana M, Sugimoto K, Nozaki M, Ueda J, Ohta T, Ohki M, Fukuda M, Takeda N, Niida H, Kato H, Shinkai Y. 2002. G9a histone methyltransferase plays a dominant role in euchromatic histone H3 Lys9 methylation and is essential for early embryogenesis. Genes Dev 16:1779–1791.

Tamaru H, Selker EU. 2001. A histone H3 methyltransferase controls DNA methylation in *Neurospora crassa*. Nature 414:277–283.

Tsai T-F, Jiang Y, Bressler J, Armstrong D, Beaudet AL. 1999. Paternal deletion from *Snrpn* to *Ube3a* in the mouse causes hypotonia, growth retardation, and partial lethality and provides evidence for a gene contributing to Prader–Willi syndrome. Hum Mol Genet 8:1357–1364.

Umlauf D, Goto Y, Cao R, Cerqueira F, Wagschal A, Zhang Y, Feil R. 2004. Imprinting along the *Kcnq1* domain on mouse chromosome 7 involves repressive histone methylation and recruitment of Polycomb group complexes. Nat Genet 36:1296–1300.

Weksberg R, Smith A, Squire J, Sadowski P. 2003. Beckwith–Wiedemann syndrome demonstrates a role for epigenetic control of normal development. Hum Mol Genet 12:R61–R68.

Xin Z, Allis CD, Wagstaff J. 2001. Parent-specific complementary patterns of histone H3 Lys9 and Lys4 methylation at the Prader–Willi imprinting center. Am J Hum Genet 69:1389–1394.

Xin Z, Tachibana M, Guggiari M, Heard E, Shinkai Y, Wagstaff J. 2003. Role of histone methyltransferase G9a in CpG methylation of the Prader–Willi syndrome imprinting center. J Biol Chem 278:14996–15000.

Yamasaki K, Joh K, Ohta T, Masuzaki H, Ishimaru T, Mukai T, Niikawa N, Ogawa M, Wagstaff J, Kishino T. 2003. Neurons but not glial cells show reciprocal imprinting of sense and antisense transcripts of *Ube3a*. Hum Mol Genet 12:837–847.

Yatsuki H, Joh K, Higashimoto K, Soejima H, Arai Y, Wang Y, Hatada I, Obata Y, Morisaki H, Zhang Z, Nakagawachi T, Satoh Y, Mukai T. 2002. Domain regulation of imprinting cluster in *Kip2/Lit1* subdomain on mouse chromosome 7F4/F5: Large-scale DNA methylation analysis reveals that DMR-*Lit1* is a putative imprinting control region. Genome Res 12:1860–1870.

Zhang P, Liegeois NJ, Wong C, Finegold M, Hou H, Thompson JC, Silverman A, Harper JW, DePinho RA, Elledge SJ. 1997. Altered cell differentiation and proliferation in mice lacking *p5KIP2* indicates a role in Beckwith-Wiedemann syndrom. Nature 387:151–158.

Zwart R, Sleutels F, Wutz A, Schinkel AH, Barlow DP. 2001. Bidirectional action of the *Igf2r* imprint control element on upstream and downstream genes. Genes Dev 15:2361–2366.

Cisplatin represses transcriptional activity from the minimal promoter of the O^6-methylguanine methyltransferase gene and increases sensitivity of human gallbladder cancer cells to 1-(4-amino-2-methyl-5-pyrimidinyl) methyl-3-2-chloroethyl)-3-nitrosourea

KEN SATO[1], YOSHIHIKO KITAJIMA[1], TETSUJI NAKAGAWACHI[2], HIDENOBU SOEJIMA[2], ATSUSHI MIYOSHI[1], YASUO KOGA[1] and KOHJI MIYAZAKI[1]

[1]Department of Surgery and [2]Division of Molecular Biology and Genetics, Department of Biomolecular Sciences, Saga University Faculty of Medicine, Saga, Japan

Received October 26, 2004; Accepted December 20, 2004

Abstract. O^6-methylguanine methyltransferase (MGMT) repairs O^6-alkylguanine in cellular DNA introduced by the clinically used alkylating drug 1-(4-amino-2-methyl-5-pyrimidinyl) methyl-3-(2-chloroethyl)-3-nitrosourea (ACNU). Thus, cancer cells with MGMT expression are resistant to ACNU treatment. Cisplatin has been reported to suppress MGMT expression; however, the molecular mechanism by which cisplatin reduces MGMT expression remains to be elucidated. Using gallbladder cancer cells (KMG-C) expressing MGMT, we analyzed whether a low dose of cisplatin suppresses MGMT expression, followed by an enhanced drug effect of ACNU *in vitro* and *in vivo*. We also investigated the promoter region critical for the transcriptional repression of MGMT gene by cisplatin using 5 deletion mutants in reporter promoter assays. In RT-PCR analysis, the expression of MGMT mRNA in KMG-C cells was dose- and time-dependently repressed. Drug sensitivity to ACNU was increased 2-fold by pretreatment with cisplatin, compared with only ACNU treatment, in MTT assays as well as tumor-bearing nude mice. Although the 5'-flanking region is deleted as far as -69 bp upstream of the transcription start site, cisplatin dose dependently inhibited luciferase activity. However, cisplatin did not cause such repression when 59 bp region from -69 to -10 bp was deleted. We confirmed that cisplatin enhanced sensitivity to ACNU in KMG-C cells expressing MGMT both *in vitro* and *in vivo*. Furthermore, a low dose of cisplatin repressed the transcription of the MGMT promoter. The 59 bp region in the MGMT promoter was crucial for repression by cisplatin. These results might form the basis of a chemotherapeutic strategy involving alkylating agents via prior cisplatin-induced biochemical modulation.

Correspondence to: Dr Kohji Miyazaki, Department of Surgery, Saga University Faculty of Medicine, Nabeshima 5-1-1, Saga 849-8501, Japan
E-mail: miyazak2@post.saga-med.ac.jp

Key words: O^6-methylguanine methyltransferase (MGMT), cisplatin, promoter, 1-(4-amino-2-methyl-5-pyrimidinyl) methyl-3-(2-chloroethyl)-3-nitrosourea (ACNU), gallbladder cancer

Introduction

Alkylating agents are highly reactive molecules that cause DNA mutation leading to cell death (1-3) and those such as N-methyl-N-nitrosourea (MNU) and N-methyl-N'-nitroso-guanidine (MNNG) introduce methylation at the O^6 position of guanine in cellular DNA (1,4). O^6-methylguanine-DNA methyltransferase (MGMT) specifically removes the methyl group by transferring to a cysteine residue in a single-step reaction (1,5,6). Among the alkylating agents designed for use in cancer chemotherapy, CENUs such as 1-(4-amino-2-methyl-5-pyrimidinyl) methyl-3-(2-chloroethyl)-3-nitrosourea (ACNU), 1,3-bis(2-chloroethyl)-1-nitrosourea (BCNU) and 1-(2-chloroethyl)-3-cyclohexyl-1-nitrosourea (CCNU) introduce O^6-chroloethylguanine into DNA. In addition, MGMT can also remove O^6-chloroethyl groups from DNA (7-9), and human brain tumors such as glioma and glioblastoma that express MGMT are resistant to ACNU (10,11).

Recently, drugs that deplete MGMT activity are used clinically to overcome resistance to chemotherapy with alkylating agents. For instance, drugs such as streptozotocin, dacarbazine (DTIC) and fotemustine directly or indirectly reduce MGMT activity (12-16). However, these drugs have serious side effects that limit their clinical application in cancer patients. O^6-benzylguanine (O^6-BG) is known to repress MGMT activity and thus enhances the subsequent effects of alkylating agents such as 1,3-bis(2-chloroethyl)-1-nitrosourea (BCNU) *in vitro* and *in vivo* (17-20). The low molecular weight MGMT substrate, BG, binds readily to the

same cysteine residue on MGMT that is used for alkyl group transfer and inactivates the MGMT protein (21,22). Phase II trials of a combination of O^6-BG and alkylating agents are presently ongoing.

Current reports have demonstrated that cisplatin reduces MGMT activity and enhances the efficacy of alkylating agents such as temozolomide (TMZ) and DTIC (23-25). However, the mechanism by which cisplatin attenuates MGMT activity remains to be understood.

Cisplatin is one of the most widely used cancer chemotherapeutic drugs. Although cisplatin reacts with DNA as well as RNA and protein, DNA is believed to be the principal site of cisplatin action (26,27).

Here, we designed a modulated ACNU chemotherapy mediated via reduced MGMT expression through low-dose cisplatin treatment in the gallbladder (GB) cancer cell line KMG-C. We initially performed RT-PCR to assess whether MGMT expression in KMG-C is repressed by a low dose of cisplatin. We then compared the effects of the alkylating agent, ACNU, alone and in combination with cisplatin using the MTT assay. We also assessed the *in vivo* effect of cisplatin + ACNU using tumor-bearing nude mice. To address how cisplatin depletes the MGMT expression, we performed reporter assays in KMG-C cells transiently transfected with an MGMT promoter-luciferase plasmid. We constructed 5 reporter plasmids with various deletions in the MGMT promoter region and attempted to define the DNA region that is crucial for cisplatin-dependent repression of the MGMT promoter.

Materials and methods

Cell line. The gallbladder cancer cell line KMG-C with MGMT expression was provided by Dr H. Yano (Department of Pathology, Kurume University, Japan). KMG-C cells were cultured in Williams' medium E (W/E, ICN Biomedicals Inc., Costa Mesa, CA), supplemented with 10% inactivated FBS (JRH Biosciences, Lenexa, KS), 2 mM glutamine, 100 μg/ml kanamycin and 20 μg/ml tetracycline hydrochloride and incubated at 37°C in a humidified atmosphere of 5% CO_2 in air.

Drugs. ACNU, kindly supplied by Sankyo Co. (Tokyo, Japan), was dissolved in distilled water immediately before use. Cisplatin was purchased from Nihon Kayaku Co. (Tokyo, Japan) and diluted in medium before use.

Cytotoxicity assays. Drug cytotoxicity was determined by the MTT assay using the Cell Titer96 Non-Radioactive Cell Proliferation Assay kit (Promega, Madison, WI). KMG-C cells ($8x10^3$/well) were seeded on 96-well culture plates in triplicate. After 24 h, the cells were exposed to 5 μM cisplatin for 12 h. The medium was then removed and the cells were washed with PBS. Finally, KMG-C cells were exposed to 50 μM ACNU for 2 h. The cells were washed in PBS, fresh medium was added, then 20 μl of [3(4,5-dimethylthiazol-2-yl)-2,5-diphenyltetrazolium bromide] (MTT) was added to the cultured cells. After 4 h, reaction was stopped by adding solubilization/stop solution. Absorbance at 530 nm was measured using a multiwell plate reader (CS9300PC, Shimadzu Co., Kyoto, Japan). Data are presented as means ± S.D. of 3 individual experiments.

Reverse transcriptase (RT)-PCR. KMG-C cells were incubated with 2.5, 5 and 10 μM cisplatin. After 12 and 24 h, total RNA was isolated using Isogen (Nippongene, Toyama, Japan). Expression of MGMT mRNA after treatment with cisplatin was analyzed by RT-PCR using the RNA LA PCR™ kit (AMV) Ver. 1.1 (Takara Biomedicals, Tokyo, Japan). Total RNA (1 μg) was used for first-strand cDNA synthesis. The resultant cDNA was amplified by PCR for 30 cycles of 94°C for 1 min, 56°C for MGMT and 60°C for GAPDH for 30 sec, and 72°C for 90 sec. The primers for MGMT, and GAPDH were as follows: MGMT forward, 5'-CACGAAATAAAG CTCCTGGG-3'; MGMT reverse, 5'-CTGCCAGGGCTG CTAATTGC-3'; GAPDH forward, 5'-TGGTATCGTGGAA GGACTCATGAC-3'; GAPDH reverse, 5'-ATGCCAGT GAGCTTCCCGTTCAGC-3'. The proposed sizes of PCR products were 282 bp for MGMT and 189 bp for GAPDH, which was simultaneously amplified in each sample as the internal marker. All reactions were repeated twice. For quantitative analysis, PCR products were densitometrically evaluated using the LAS 1000 plus system (Fujifilm, Japan).

In vivo experiment. Female athymic BALB/cA Jcl mice (nu/nu, 5 weeks old) obtained from Nihon Crea Co. (Osaka, Japan) were maintained under specific-pathogen-free conditions, and given γ-irradiated food and autoclaved water. Approximately $1x10^6$ cells of KMG-C were subcutaneously injected into both flanks of 18 mice (36 tumors). When tumor xenografts became palpable, the mice were weighed and the tumors were measured twice each week in 2 perpendicular dimensions using a caliper. Tumor volume (V) was determined using the formula (28,29) $V=0.5xaxb^2$, where a is the longer, and b is the shorter of the 2 dimensions (mm). When the xenograft volume reached about 400 mm^3, the mice were separated into the following groups of 3 mice (6 tumors): i) control (distilled water); ii) 50 mg/kg ACNU; iii) 12.5 mg/kg cisplatin; iv) 25 mg/kg cisplatin; v) 12.5 mg/kg cisplatin + 50 mg/kg ACNU and vi) 25 mg/kg cisplatin + 50 mg/kg ACNU. Both drugs were suspended in 0.3 ml of distilled water. Cisplatin was intraperitoneally injected into the mice, and then ACNU was injected 24 h later. The control was an intraperitoneal injection of 0.3 ml of distilled water. This procedure was repeated three times at 1-week intervals. The growth of each tumor was assessed as relative volume (RVn = Vn/Vo), where Vo is initial tumor volume at the time of the first injection (day 0), and Vn is the volume on the n^{th} day. The relative growth rate was estimated as the ratio of treated tumors (Tn) to controls (Cn): Tn/Cnx100%. The growth inhibition rate (IR) was estimated using the formula IR = (1-Tn/Cn)x100% (28). The acute toxicity of drugs was estimated from the amount of weight lost by the mice.

Construction of MGMT promoter plasmid. A 795-bp DNA fragment (PstI-XhoI) spanning the 5'-flanking region and first intron of the MGMT gene inserted into PGV-B (Toyo Beanet Co., Tokyo, Japan) was obtained from Dr T. Nakagawachi (30). PstI is located 570 bp upstream from the transcription start site (+1), whereas XhoI is at 224 bp downstream. The

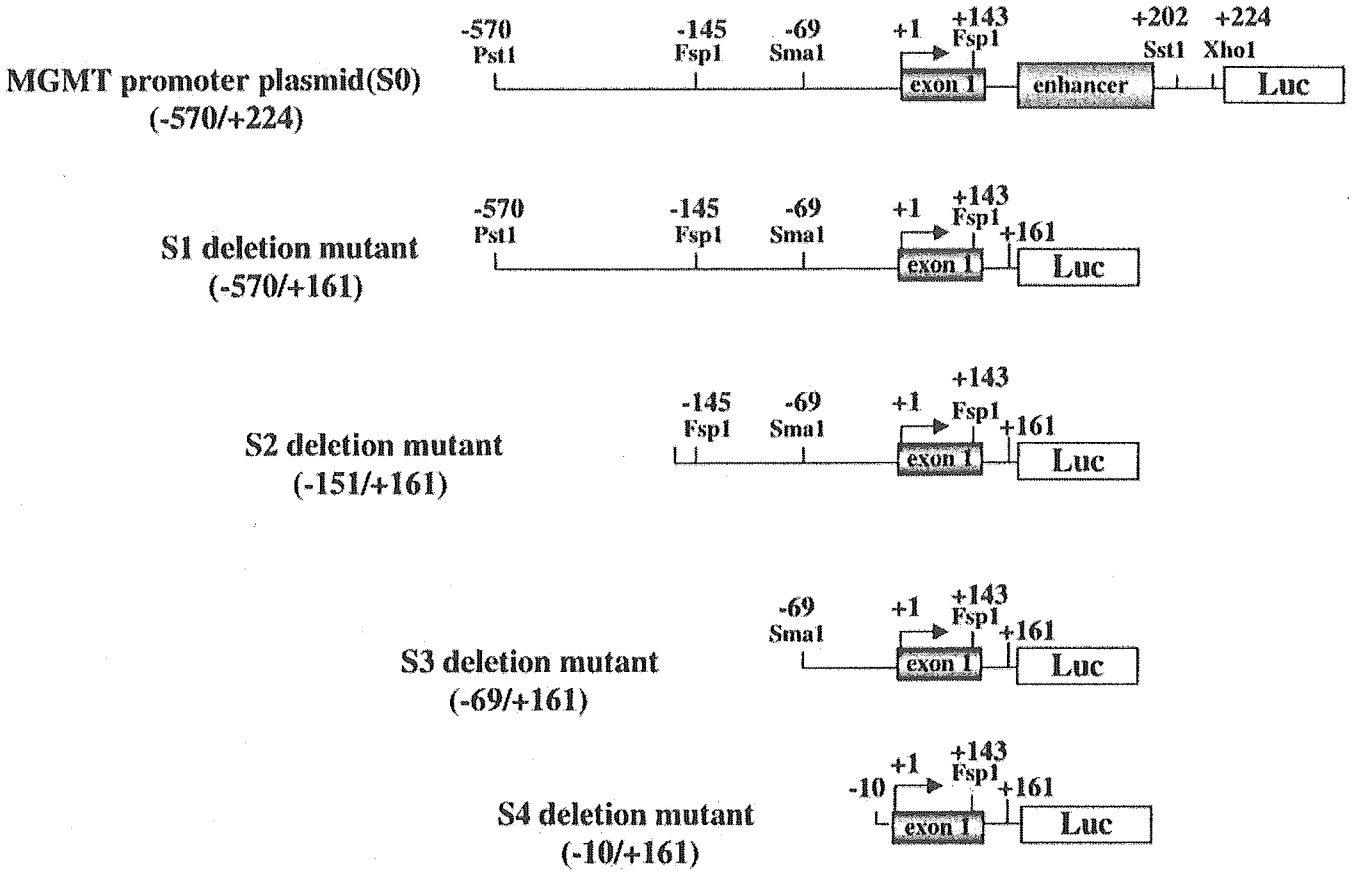

Figure 1. Schematic diagram of MGMT promoter plasmid (S0) and four deletion mutants (S1-S4). Arrow, transcription start site numbered as +1. Positions of various restriction sites are indicated as base pairs (bp) from transcription initiation site (+1). Promoter regions spanning -570 to +224 for S0, -570 to +161 for S1, -151 to +161 for S2, -69 to +161 for S3 and -10 to +161 for S4 were attached to luciferase gene in pGL3-basic.

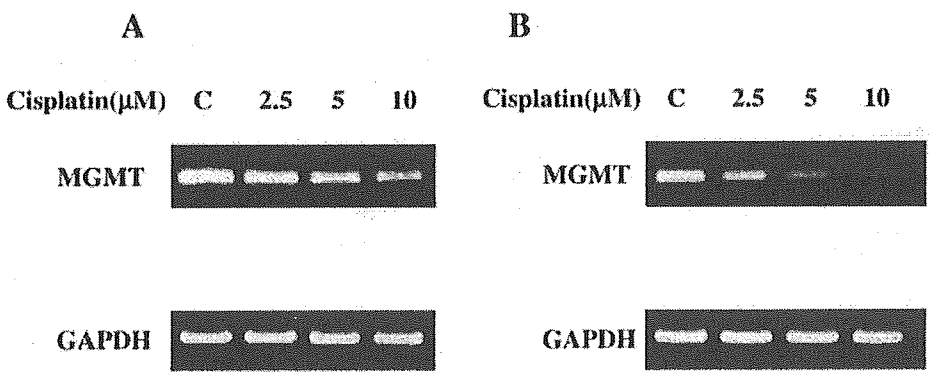

Figure 2. RT-PCR analysis of MGMT expression in KMG-C cells under cisplatin exposure. Cells were incubated under 0 (control), 2.5, 5, or 10 μM cisplatin for (A) 12 or (B) 24 h. Expression of GAPDH was evaluated under same conditions as internal control.

MGMT promoter fragment was subcloned upstream of the luciferase gene of the pGL3-BasicVecter (Promega) to construct pGL3-S0 (Fig. 1).

Construction of promoter reporter plasmid with various deletions. We constructed several reporter plasmids with various deletions in the MGMT promoter region S0 (-570/+224) and named them S1 (-570/+161), S2 (-151/+161), S3 (-69/+161) and S4 (-10/+161) (Fig. 1). Three deletion mutants (S1, S2 and S4) were generated by PCR. To construct S1, S2 and S4, PCR reactions were performed using Advantage™-GC Genomic PCR kits (Clontech) for 25 cycles of 94°C for 30 sec and 68°C for 3 min. We included 1 μg of pGL3-S0 as template DNA, the forward primers 5'-CTGCAGCCCCTGG ACGGCATC-3' (-570 to -550 bp) for S1, 5'-GGATGCGCA GACTGCCTCAGG-3' (-151 to -131 bp) for S2 and 5'-TTTT CTCAGGTCCTCGGCTCC-3' (-10 to +11) for S4 and the reverse primer 5'-CCAAGTCGCAAACGGTGCGCA-3' (+140 to +161) for S1, S2 and S4. After PCR amplification, the PCR products were then inserted into the PSTBlue-1 blunt-ended

Table I. Quantitative assessment of MGMT mRNA in KMG-C cells under cisplatin exposure at various concentrations.

	Control	2.5 μM	5 μM	10 μM
KMG-C				
12 h	1	0.75	0.55	0.44
24 h	1	0.65	0.36	0.13

vector (Novagen, Inc., Darmstadt, Germany). The orientation and sequence of the inserts were verified using the Big Dye Terminator Cycle Sequencing Ready Reaction (Perkin Elmer Applied Biosystems Division, Foster City, CA) and analyzed on an ABI Prism 310 (Perkin Elmer). The mutants in PSTBlue-1 were digested between the KpnI/HindIII restriction site and inserted into the KpnI/HindIII site of pGL3-Basic. To construct the S3 deletion mutant, the S2 deletion mutant was digested between Eco105I and SmaI to remove 82 bp (-151 to -70), and self-ligated.

Transient transfection and reporter promoter assays. KMG-C cells ($5x10^5$) were seeded onto 6-well plates and incubated overnight. DNA (1 μg) of reporter plasmids, S0, S1, S2, S3, S4 or negative control plasmid pGL-3 Basic were cotransfected with 0.5 μg of the ß-galactosidase expression plasmid pCMV (Clontech) into KMG-C cells using Lipofectamine (Life Technologies, Inc.). The medium was changed 4 h later. At 24 h after transfection, KMG-C cells were exposed to 2.5 and 5 μM cisplatin for another 24 h. The cells were lysed in 5X reporter lysis buffer (Promega). The activities of luciferase in the cell lysates were measured using a luciferase assay kit (Promega) and normalized by those of ß-gal. Transfection was performed in triplicate and the experiments were repeated at least three times.

Statistical analysis. The sensitivity of cells to cisplatin, ACNU and cisplatin + ACNU combination was assessed statistically using Fisher's PLSD method. Differences in the tumor volumes of treated vs. control mice on days 14 and 21 were statistically analyzed by using Student's t-test. Statistical differences in relative luciferase activities between the control and cisplatin 5 μM groups of S0-S4 deletion mutants were also analyzed using Student's t-test.

Results

Cisplatin repressed MGMT expression. Fig. 2 showed that MGMT mRNA expression in KMG-C cells was dose- and time-dependently decreased. In contrast, GAPDH expression was not affected by cisplatin exposure in either cell line. The quantitative expression of MGMT mRNA is densitometrically estimated and shown in Table I. The density of the MGMT band was diminished to 0.75, 0.55 and 0.44 after 12 h exposure to 2.5, 5 and 10 μM cisplatin, respectively. After 24 h exposure, these values were decreased to 0.65, 0.36 and 0.13, respectively.

Cisplatin enhanced ACNU sensitivity. We compared the effects of 5 μM cisplatin, 50 μM ACNU and a combination of both

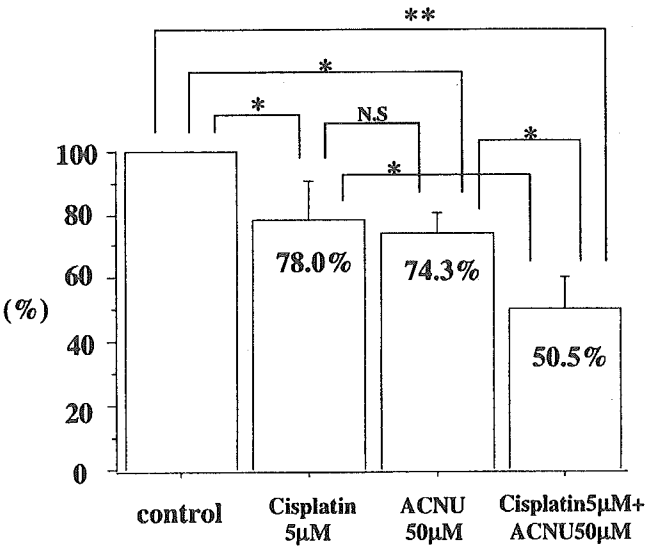

Figure 3. Drug sensitivity of KMG-C cells to ACNU, cisplatin and cisplatin + ACNU in MTT assay. Data are presented as means ± S.D. of three independent experiments. Results statistically differed among groups (*p<0.05, **p<0.001).

drugs in KMG-C cells using MTT assays (Fig. 3). Cisplatin and ACNU decreased cell viability to 78.0% and 74.3%, respectively, compared with that in the absence of drugs. Cisplatin combined with ACNU decreased the viability to 50.5% of that in the absence of drugs (p<0.0001).

Effects of cisplatin combined with ACNU against KMG-C tumors in mice. Fig. 4 shows the growth curve of KMG-C tumors in nude mice after cisplatin (12.5 and 25 mg/kg), ACNU (50 mg/kg) and cisplatin + ACNU treatments. The estimated tumor volumes and the IR values (%) on 14 and 21 days after the first treatment are summarized in Table II. As shown in Fig. 4, KMG-C xenografts in the control group rapidly proliferated. Tumors were slightly inhibited by ACNU (50 mg/kg), in which the approximate IR value (%) at day 21 was 14%. Cisplatin at 12.5 and 25 mg/kg dose dependently repressed tumor volumes, in which the IR values (%) on day 21 were 29.3% and 36.9%, respectively (Table II).

Cisplatin combined with ACNU remarkably decreased tumor volumes compared with either drug alone (Fig. 4). The IR values of 12.5 mg/kg cisplatin + ACNU and 25 mg/kg cisplatin + ACNU on day 21 were 48.2% and 52.0%, respectively (Table II).

Cisplatin repressed MGMT expression at the transcriptional level. To investigate whether cisplatin transcriptionally represses MGMT expression, we performed reporter assays using the MGMT promoter (S0) in the presence of cisplatin (Fig. 5). The relative luciferase activity from the MGMT promoter (S0) was dose-dependently repressed by cisplatin within 24 h (Fig. 5). As shown in Table III, the relative luciferase activity from the S0 promoter under 5 μM cisplatin was reduced by 36%, compared with that in the absence of cisplatin (p<0.05).

Identification of DNA element important for cisplatin-dependent suppression in MGMT promoter. To identify the cisplatin

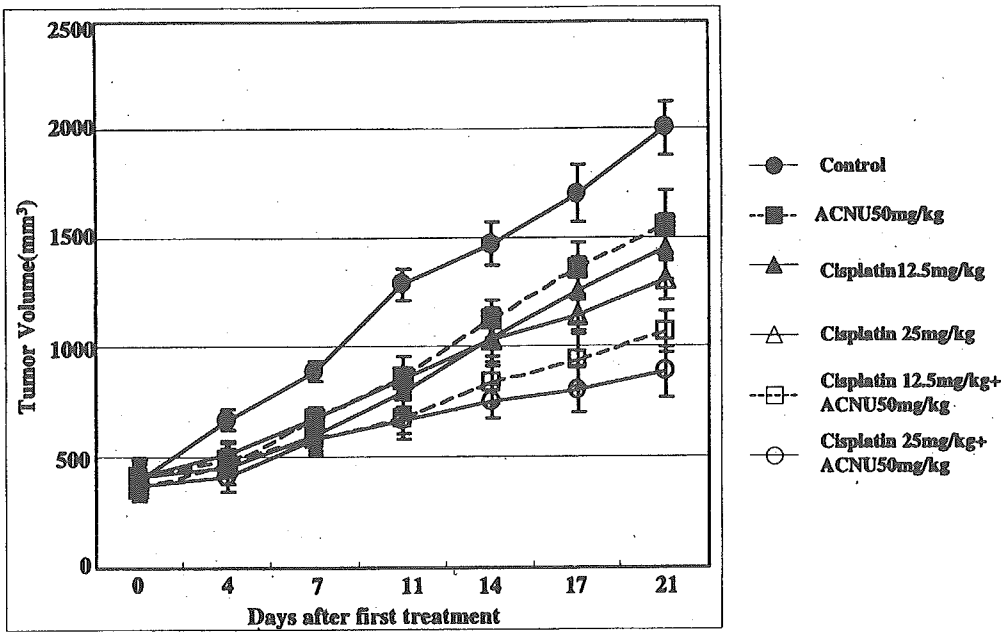

Figure 4. Growth curve of KMG-C xenografts in nude mice administered with cisplatin, ACNU and cisplatin + ACNU. The tumor volume was estimated on day 0, 4, 7, 11, 14, 17 and 21.When xenograft volume reached about 400 mm³, 18 mice were divided into groups of 3 mice (6 tumors): Control (□), ACNU 50 mg/kg (□), cisplatin 12.5 mg/kg (□), cisplatin 25 mg/kg (△), cisplatin 12.5 mg/kg + ACNU 50 mg/kg (□), cisplatin 25 mg/kg + ACNU 50 mg/kg (○). Cisplatin was intraperitoneally injected in mice. Twenty-four hours later, ACNU was subsequently injected. Controls were intraperitoneally injected with distilled water. This procedure was repeated three times at 1-week intervals. Tumor volumes are presented as means ± S.E.

Table II. Summary of tumor volumes of KMG-C xenografts on 14 and 21 days after drug administration.

Drug (mg/kg)	Tumor volume (mm³)			IR (%)	
	Days after first treatment			Days after first treatment	
	0	14	21	14	21
Control	403.9±70.5	1474.9 ± 96.4	2004.6 ± 125.3	-	-
ACNU (50)	364.2±76.4	1133.1 ± 74.2[a]	1555.7 ± 93.9[a]	14.8	13.9
Cisplatin (12.5)	415.3±56.8	1049.6 ± 86.5[a]	1457.9 ± 163.6[a]	31.7	29.3
Cisplatin (25)	417.2±84.3	1033.3 ± 93.5[a]	1307.2 ± 94.7[b]	32.1	36.9
Cisplatin (12.5) + ACNU (50)	416.8±83.3	841.4 ± 129.5[b]	1069.8 ± 152.2[c]	44.9	48.2
Cisplatin (25) + ACNU (50)	372.9±72.7	757.1 ± 78.6[c]	890.7 ± 114.9[c]	44.7	52.0

Data are presented as mean ± S.E. [a]$p<0.05$; [b]$p<0.005$; [c]$p<0.001$ vs. control group.

response region in the MGMT promoter, we constructed the 4 mutant plasmids, S1, S2, S3 and S4, in which promoter and enhancer region were variously deleted (Fig. 1). Using these mutants, the reporter promoter assays were carried out. The relative luciferase activities in the control from S1-S3 deletion mutants became gradually decreased with sequential truncations. Luciferase activities from the S1-S3 deletion mutants were also suppressed by cisplatin in the same manner as the MGMT promoter (S0) (Fig. 5). The relative luciferase activity of S1-S3 deletion mutants after cisplatin at 5 μM treatment was 53-64% of that of the control (Table III). However, the S4 deletion mutant that lacked the 59 bp region was hardly affected by cisplatin. The relative luciferase activity of S4 after exposure to 5 μM cisplatin was about 98% of that of the control (N.S.) (Table III).

Table III. Relative luciferase activity from serial reporter plasmids under 2.5 and 5 μM cisplatin exposure.

	Control	Cisplatin concentrations	
		2.5 μM	5 μM
S0	100	91.92 ± 1.09	64.91 ±1.37[a]
S1	100	92.46 ± 9.86	58.13 ±6.10[a]
S2	100	85.55 ± 12.24	59.80 ±4.77[a]
S3	100	93.20 ± 13.87	53.60 ±4.35[a]
S4	100	108.8 ± 7.47	98.0 ±5.79[b]

Data are presented as mean ± S.E. of triplicate measurements. [a]$p<0.05$; [b]N.S.

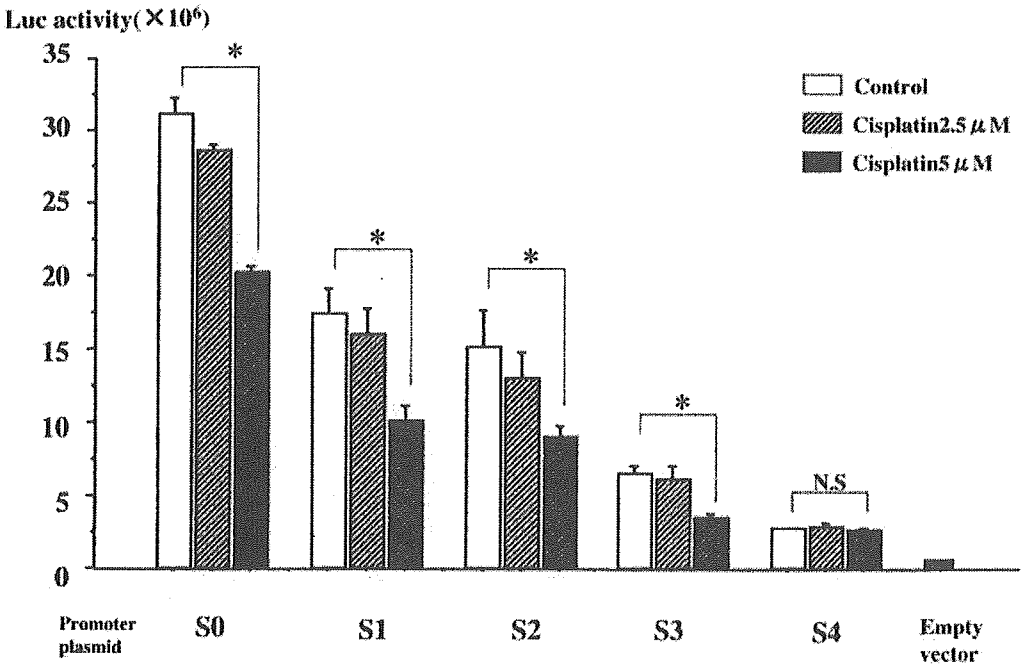

Figure 5. Luciferase activity from MGMT promoter (S0) and four deletion mutants were estimated in KMG-C cells with or without cisplatin treatment. Relative luciferase activities normalized by ß-gal activity are presented as means ± S.D. Luciferase activity of MGMT promoter (S0) was dose dependently repressed by cisplatin (*p<0.05). Activities of three deletion mutants (S1-S3) were similarly repressed by cisplatin (S1-S3, *p<0.05). However, the activity of S4 mutant was few affected by cisplatin (N.S).

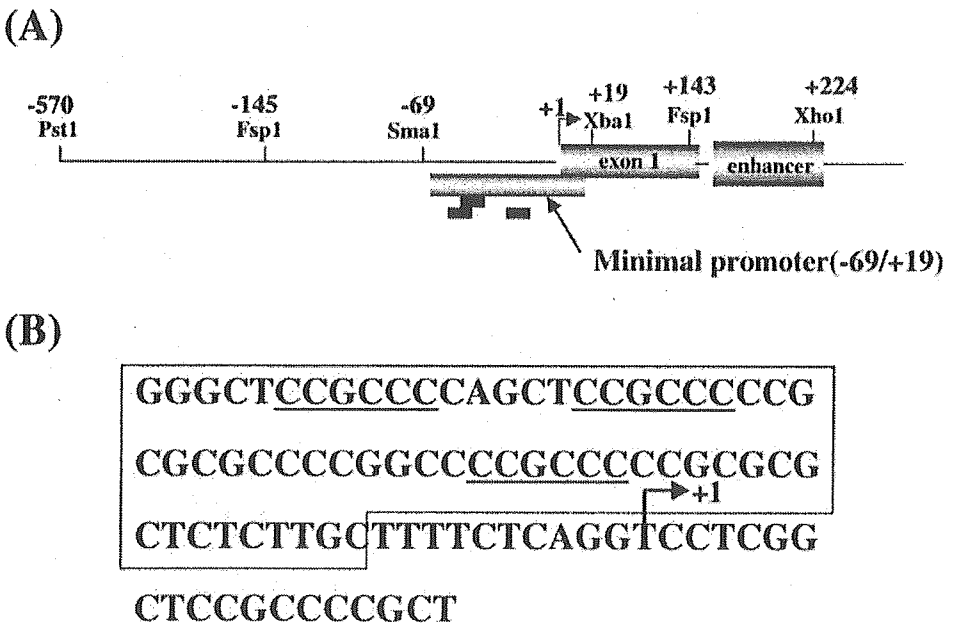

Figure 6. A, DNA fragment (PstI-XhoI) spanning the 5'-flanking region of the MGMT promoter. Minimal promoter (-69 to +19) is shown by a shadowed box. Three repeats of CCGCCC element are presented by black boxes. B, DNA sequence of MGMT minimal promoter (88 bp). Arrow, transcription start site is numbered as +1; 59 bp sequence (-69 to –10); is boxed, CCGCCC repeats in 59 bp sequence are underlined.

Discussion

Among the alkylating agents that are clinically applied to treat cancer, 1-(4-amino-2-methyl-5-pyrimidinyl) methyl-3-(2-chloroethyl)-3-nitrosourea (ACNU) is a bifunctional chloroethylnitrosourea (7). Chloroethyl groups on ACNU are transferred to guanine residues of DNA to form a cross-link with a base on the opposite strand, thereby preventing cell proliferation (7,31).

The chloroethyl group at the O^6 position of guanine in DNA can be recognized and repaired by MGMT (8,32,33). Thus, MGMT activity might be responsible for resistance to ACNU in human cancer cells. Other reports have provided evidence that Hela S3 cells deficient in MGMT expression

are far more sensitive to ACNU than the MGMT positive Hela cells (29). Mice deficient in MGMT gene have been reported to become more sensitive to ACNU than wild-type mice (31). These findings indicate that MGMT expression in human cancer confers drug resistance to alkylating agents such as ACNU. We thus inferred that effective suppression of MGMT could be an important strategy to improve the clinical effect of ACNU.

Cisplatin was reported to reduce MGMT activity (23,25). The level of MGMT mRNA in Jurkat cells is attenuated by exposure to 12.5 μM cisplatin treatment for 24 h (24). In that report, the authors speculated that MGMT expression was inhibited at the transcriptional level by cisplatin. However, no evidence has yet shown that cisplatin directly represses the promoter activity of MGMT.

In the present study, RT-PCR analysis demonstrated that MGMT expression in the GB cancer cell line, KMG-C was dramatically repressed by 5 μM cisplatin treatment. The MTT assay showed that exposure to 5 μM cisplatin for 12 h enhanced the sensitivity of KMG-C cells to ACNU. The cisplatin pretreatment was performed at another concentration (2.5, 10 μM) and exposure time (24 h). Sensitivity to ACNU was also enhanced in the cisplatin treatment (data not shown). We also confirmed that cisplatin increases the subsequent ACNU effect on tumor-bearing mice *in vivo*. These findings support the previous reports that the enhanced sensitivity to alkylating agents such as TMZ or DTIC, results from MGMT expression being reduced by cisplatin (25). We showed first evidence that MGMT expression was transcrip tionally repressed by cisplatin in reporter promoter assay.

Several investigators have demonstrated that the human 5'-flanking sequence of the MGMT gene lacks a TATA box and is GC-rich (34,35). Several cis-elements including six putative Sp1 sites and two AP-1 and AP-2 elements have been identified within 570 bp upstream of the transcription start site of the MGMT gene (34). The authors showed that the minimal promoter activity resides between SmaI (-69) and XbaI (+19) by deletion analysis (34).

The present study indicated that the 59 bp fragment (-69 to -10) between S3 to S4 might be a preferential cisplatin target, since a 5 μM concentration of the drug suppressed luciferase activity from the S3, but not the S4 deletion. Cisplatin is a bifunctional agent that forms intrastrand and interstrand cross-links on DNA and exerts drug effects. Interstrand cross-links are preferentially formed at GC sites (36). We conferred cisplatin might form interstrand cross-links around GC-rich region in MGMT promoter and disturb the transcription. If this hypothesis is correct, interstrand cross-links by cisplatin may form around GC-rich region in other gene promoters and repress the transcriptional activity. Although, mismatch repair gene hMLH1 has a GC rich promoter, its expression was little affected by cisplatin in RT-PCR analysis (data not shown). There may be another system to repress MGMT minimal promoter activity by cisplatin. Minimal promoter of MGMT gene was reported to harbor three times complementary Sp1 site CCGCCC (34), however such sequence was not observed in hMLH1 promoter (Fig. 6). Thus, the CCGCCC repeats may act as cis-element for cisplatin response as well as basal transcription.

In conclusion, the present study demonstrated that cisplatin represses MGMT expression via attenuating promoter activity. The 59 bp spanning the -69 to -10 region in the minimal promoter might include a crucial cis-element during transcriptional repression by cisplatin. We also confirmed that cisplatin increased the ACNU effect in cultured cells as well as in tumor-bearing mice, and that it was mediated by repression of the MGMT expression. These results might provide the basis for a strategy of ACNU-based chemotherapy via biochemical modulation by prior exposure to cisplatin. Such a strategy should be clinically useful against gallbladder cancer with MGMT expression.

References

1. Lindahl T, Sedgwick B, Sekiguchi M and Nakabuppu Y: Regulation and expression of the adaptive response to alkylating agents. Annu Rev Biochem 57: 133-157, 1988.
2. Esteller M, Fancillas JG, Andison E, *et al*: Inactivation of the DNA-repair gene MGMT and the clinical response of gliomas to alkylating agents. N Engl J Med 343: 1350-1354, 2000.
3. Sekiguchi M and Nakabeppu Y: Adaptive response: induced synthesis of DNA repair enzymes by alkylating agents. Trends Genet 3: 51-54, 1987.
4. Tominaga Y, Tsuzuki T, Shiraishi A, Kawate H and Sekiguchi M: Alkylation-induced apoptosis of embryonic stem cells in which the gene for DNA-repair methyltransferase had been disrupted by gene targeting. Carcinogenesis 18: 889-896, 1997.
5. Olsson M and Lindahl T: Repair of alkylated DNA in *Escherichia coli*: methyl group transfer from O^6-methylguanine to a protein cysteine residue. J Biol Chem 255: 10569-10571, 1980.
6. Kawate H, Sakumi K, Tsuzuki T, *et al*: Separation of killing and tumorigenic effects of an alkylating agents in mice defective in two of the DNA repair genes. Proc Natl Acad Sci USA 95: 5116-5120, 1998.
7. Pegg AE, Dolan ME and Moschel RC: Structure, function, and inhibition of O^6-methylguanine-DNA methyltransferase. Prog Nucleic Acid Res Mol Biol 51: 167-223, 1995.
8. Robins P, Harris AL, Goldsmith I and Lindahl T: Cross-linking of DNA induced by chloroethylnitrosourea is prevented by O^6-methylguamnine-DNA methyltransferase. Nucleic Acids Res 11: 7743-7758, 1983.
9. Tsujimura T, Zhang YP, Fujio C, *et al*: O^6-methylguanine methyltransferase activity and sensitivity of Japanese tumor cell strains to 1-(4-amino-2-methyl-5-pyrimidinyl) methyl-3-(2-chloroethyl)-3-nitrosourea hydrochloride. Jpn J Cancer Res 78: 1207-1215, 1987.
10. Nagane M, Asai A, Shibui S, Nomura K, Matsutani M and Kuchino Y: Expression of O^6-methylguamnine-DNA methyltransferase and chloroethylnitrosourea resistance of human brain tumors. Jpn J Clin Oncol 22: 143-149, 1992.
11. Mineura K, Izumi I, Watanabe K and Kowada M: Influence of O^6-methylguamnine-DNA methyltransferase activity on chloroethylnitrosourea chemotherapy in brain tumors. Int J Cancer 55: 76-81, 1993.
12. Brent TP: Inactivation of purified human O^6-alkylguanine-DNA alkyltransferase by alkylating agents or alkylated DNA. Cancer Res 46: 2320-2323, 1986.
13. Gerson SL: Modulation of human lymphocyte O^6-alkylguanine-DNA alkyltransferase by streptozocin *in vivo*. Cancer Res 49: 3134-3138, 1989.
14. Lee SM, Thatcher N and Margison GP: O^6-alkylguanine-DNA alkyltransferase depletion and regeneration in human peripheral lymphocytes following dacarbazine and fotemustine. Cancer Res 51: 619-623, 1991.
15. Pieper RO, Futcher BW, Dong Q and Erickson LC: Effects of streptozocin/bis-chloroethylnitrosourea combination therapy on O_6-methylguanine DNA methyltransferase activity and mRNA levels in HT-29 cells *in vitro*. Cancer Res 51: 1581-1585, 1991.
16. Dolan ME and Mitchell RB: Effect of temozolomide and dacarbazine on O^6-alkyllguamnine-DNA alkyltransferase activity and sensitivity of human tumor cells and xenografts to 1,3-bis(2-chloroethyl)-1-nitrosourea. Cancer Chemother Pharmacol 32: 59-63, 1993.
17. Dolan ME and Pegg AE: O^6-benzylguanine and its role in chemotherapy. Clin Cancer Res 3: 837-847, 1997.

18. Schilsky RL, Dolan ME, Bertucci D, *et al*: Phase I clinical and pharmacological study of O^6-benzylguanine followed by carmustine in patients with advanced cancer. Clin Cancer Res 6: 3025-3031, 2000.
19. Dolan ME, Posner M, Karrison T, *et al*: Determination of the optimal modulatory dose of O^6-benzylguanine in patients with surgically respectable tumors. Clin Cancer Res 8: 2519-2523, 2002.
20. Kokkinakis DM, Ahmed MM, Chendi D, Moschel RC and Pegg AE: Sensitization of pancreatic tumor xenografts to carmustine and temozolomide by inactivation of their O^6-methylguanine DNA methyltransferase with O^6-benzylguanine or O^6-benzyl-2'-deoxyguanosine. Clin Cancer Res 9: 3801-3807, 2003.
21. Dolan ME, Moschel RC and Pegg AE: Depletion of mammalian O^6-alkylguanine DNA alkyltransferase activity by O^6-benzylguanine provides a means to evaluate the role of this protein in protection against carcinogenic and therapeutic alkylating agents. Proc Natl Acad Sci USA 87: 5368-5372, 1990.
22. Pegg AE, Boosalis M, Samson L, Moschel RC, Byers TL, Swenn K and Dolan ME: Mechanism of inactivation of human O^6-alkylguanine DNA alkyltransferase by O^6-benzylguanine. Biochemistry 32: 11998-12006, 1993.
23. Wang LG and Setlow RB: Inactivation of O^6-alkylguanine-DNA alkyltransferase in Hela cells by cisplatin. Carcinogenesis 10: 1681-1684, 1989.
24. D'Atri S, Graziani G, Lacal PM, *et al*: Attenuation of O^6-methylguanine DNA methyltransferase activity and mRNA levels by cisplatin and temozolomide in Jurkat cells. J Pharmacol Exp Ther 294: 664-671, 2000.
25. Piccioni D, D'Atri S, Papa G, Caravita T, Franchi A, Bonmassar E and Graziani G: Cisplatin increases sensitivity of human leukemic blasts to triazene compounds. J Chemother 7: 224-228, 1995.
26. Munchhausen LL and Rahn RO: Biologic and chemical effects of cis-dichlorodiamineplatinum (II). Cancer Chem Rep 59: 643-646, 1975.
27. Rosenberg B: Fundamental studies with cisplatin. Cancer 55: 2303-2316, 1984.
28. Geran RI, Greenberg NH, MacDonald MM, Schumacher AM and Abbort BJ: Protocols for screening chemical agents and natural products against animal tumors and other biological systems. Cancer Chemother Rep 3: 51-61, 1972.
29. Fujio C, Hae RC, Tujimura T, Ishizaki K, Kitamura H and Ikenaga M: Hypersensitivity of human tumor xenografts lacking O^6-alkylguanine-DNA alkyltransferase to the anti-tumor agent 1-(4-amino-2-methyl-5-pyrimidinyl) methyl-3-(2-chloroethyl)-3-nitrosourea. Carcinogenesis 10: 351-356, 1989.
30. Tetsuji N, Hidenobu S, Takeshi U, *et al*: Silencing effect of CpG island hypermethylation and histone modifications on O^6-methylguanine-DNA methyltransferase (MGMT) gene expression in human cancer. Oncogene 22: 8835-8844, 2003.
31. Shiraishi A, Sakumi K and Sekiguchi M: Increased susceptibility to chemotherapeutic alkylating agents of mice deficient in DNA repair methyltransferase. Carcinogenesis 21: 1879-1883, 2000.
32. Erickson LC, Laurent G, Sharkey NA and Kohn KW: DNA cross-linking and monoadduct repair in nitrosourea-treated human tumour cells. Nature 288: 727-729, 1980.
33. Brent TP: Suppression of cross-link formation in chloroethylnitrosourea-treated DNA by an activity in extracts of human leukemic lymphoblasts. Cancer Res 44: 1887-1892, 1984.
34. Harris LC, Potter PM, Tano K, Shiota S, Mitra S and Brent TP: Characterization of the promoter region of the human O^6-methylguanine-DNA methyltransferase gene. Nucleic Acids Res 19: 6163-6167, 1991.
35. Nakatsu Y, Hattori K, Hayakawa H, Shimizu K and Sekiguchi M: Organization and expression of the human O^6-methylguanine-DNA methyltransferase. Mutat Res DNA Repair 293: 119-132, 1993.
36. Lemaire MA, Schwartz A, Rahmouni AR and Leng M: Interstrand cross-links are preferentially formed at the d(GC) sites in the reaction between cis-diamminedichloroplatinum (II) and DNA. Proc Natl Acad Sci USA 88: 1982-1985, 1985.

Published online May 11, 2005

2650–2660 Nucleic Acids Research, 2005, Vol. 33, No. 8
doi:10.1093/nar/gki555

ZAC, LIT1 (KCNQ1OT1) and $p57^{KIP2}$ (CDKN1C) are in an imprinted gene network that may play a role in Beckwith–Wiedemann syndrome

Takahiro Arima*, Tetsuya Kamikihara, Toshirou Hayashida[1], Kiyoko Kato, Toshiaki Inoue[2], Yasuaki Shirayoshi[1], Mitsuo Oshimura[3], Hidenobu Soejima[4], Tunehiro Mukai[2] and Norio Wake

Department of Reproductive Physiology and Endocrinology, Medical Institute of Bioregulation, Kyusyu University, 4546, Tsurumihara, Beppu, Oita 874-0838, Japan, [1]Department of Molecular and Cell Genetics, [2]Department of Human Genome Science (Kirin Brewery), [3]Department of Biomedical Science, Institute of Regenerative Medicine and Biofunction, Graduate School of Medical Science, Tottori University, Nishi-cho 86, Yonago, Tottori 683-8503, Japan and [4]Department of Biochemistry, Saga Medical School, 5-1-1 Nabeshima, Saga 849-8501, Japan

Received February 11, 2005; Revised and Accepted April 18, 2005

ABSTRACT

Loss of genomic imprinting is involved in a number of developmental abnormalities and cancers. *ZAC* is an imprinted gene expressed from the paternal allele of chromosome 6q24 within a region known to harbor a tumor suppressor gene for several types of neoplasia. $p57^{KIP2}$ (*CDKN1C*) is a maternally expressed gene located on chromosome 11p15.5 which encodes a cyclin-dependent kinase inhibitor that may also act as a tumor suppressor gene. Mutations in *ZAC* and $p57^{KIP2}$ have been implicated in transient neonatal diabetes mellitus (TNDB) and Beckwith–Wiedemann syndrome, respectively. Patients with these diseases share many characteristics. Here we show that mouse *Zac1* and $p57^{Kip2}$ have a strikingly similar expression pattern. ZAC, a sequence-specific DNA-binding protein, binds within the CpG island of *LIT1 (KCNQ1OT1)*, a paternally expressed, anti-sense RNA thought to negatively regulate $p57^{KIP2}$ in *cis*. ZAC induces *LIT1* transcription in a methylation-dependent manner. Our data suggest that *ZAC* may regulate $p57^{KIP2}$ through *LIT1*, forming part of a novel signaling pathway regulating cell growth. Mutations in *ZAC* may, therefore, contribute to Beckwith–Wiedemann syndrome. Furthermore, we find changes in DNA methylation at the *LIT1* putative imprinting control region in two patients with TNDB.

INTRODUCTION

Genomic imprinting is a gamete-specific modification that results in the differential expression of the two parental alleles in somatic cells (1,2). Mutations that affect the epigenetic status of imprinted loci are involved in a number of human diseases, developmental abnormalities and malignant tumors indicating a general role for imprinted genes in mammalian development (3). Several imprinted genes, including *INS2*, $p57^{KIP2}$ (*CDKN1C*), *GNAS*, *RASGRF1*, *MASH2* and *ZAC* play a role in regulating the cell cycle (4).

ZAC was originally identified, along with *p53*, in a functional screen for factors that induce expression of the pituitary adenylate cyclase activating polypeptide (*PACAP*) type I receptor gene (5). ZAC encodes a zinc finger protein and is expressed only from the paternal allele with the maternal allele silent and methylated (6–8). Mutations in *ZAC* are thought to play a role in transient neonatal diabetes mellitus (TNDM). The gene maps to 6q24–25, a region implicated in the origin of several cancers (9–12). Abdollahi *et al.* (13) reported a high incidence of allelic loss at this chromosomal region in ovarian cancers. In addition, they independently cloned as *Lot1* (Lost on transformation), the rat ortholog of *ZAC*, from rat ovarian surface epithelial cells that spontaneously transform *in vitro*.

ZAC exhibits a tumor suppressor activity characterized by induction of apoptosis and G1 arrest. This proceeds independently of known cell cycle control proteins, such as pRB, p21, p27 and p16 (5). Nevertheless, ZAC shares a number of similar functions to p53. Both proteins regulate the cell cycle, apoptosis and nuclear receptors. They interact physically and functionally with CBP and p300 that serve as integrators of multiple signaling pathways (14,15). Both p53 and ZAC are

*To whom correspondence should be addressed. Tel: +81 977 271660; Fax: +81 977 271661; Email: tarima@tsurumi.beppu.kyushu-u.ac.jp

sequence-specific DNA-binding proteins and can act as transcriptional co-factors for other transcriptional activator proteins (16,17). Recently, ZAC was shown to specifically enhance the activity of p53-responsive promoters in cells expressing wild-type p53 (18). It is, therefore, possible that ZAC may act as a transcription factor with a similar mode of action to p53.

Three types of mutations have been shown to result in TNDM; paternal uniparental isodisomy of chromosome 6, paternally inherited duplication of 6q24 and a methylation defect at a CpG island overlapping exon 1 of *ZAC/HYMAI* (19). We showed that this CpG island is differentially methylated (20). The region is unmethylated in sperm but methylated in oocytes, a difference that persists between parental alleles throughout pre- and post implantation development suggestive of an imprint control region (ICR). There is a region within this putative ICR that exhibits a high degree of homology between mouse and human that acts as a strong transcriptional repressor when methylated. Loss of methylation at 8 CpG sites within this region was seen in five of six TNDM patients studied with a normal karyotype. We proposed that the DMR adjacent to *ZAC* may regulate expression of imprinted genes within the domain, and that epigenetic or genetic mutations of this region result in TNDM by affecting expression of *ZAC* in the pancreas and/or the pituitary (20). This is supported by the recent findings that mice overexpressing human ZAC from a transgene show impaired development of the endocrine pancreas and impaired β-cell function (21). ZAC may mediate its actions through transcriptional regulation of the *PACAP* type I receptor gene which is a potent insulin secretagogue and an important mediator of autocrine control of insulin secretion in the pancreatic islet (20).

During our studies on mouse *Zac1* (20), we noted a similarity in the expression pattern of *Zac1* with a second imprinted gene, $p57^{Kip2}$ (*Cdkn1c*), hereafter referred to as $p57^{Kip2}$. $p57^{KIP2}$ is a maternally expressed gene that encodes a cyclin-dependent kinase inhibitor. The protein inhibits all G_1 cyclin/Cdk complexes and negatively regulates cell proliferation, acting downstream of p53. Like *ZAC*, $p57^{KIP2}$ may also act as a tumor suppressor through its role in regulating the cell cycle (22–24). $p57^{KIP2}$ is located on human chromosome 11p15.5, a region implicated in both sporadic cancers and Beckwith–Wiedemann syndrome (BWS), a familial cancer syndrome, making it a candidate tumor suppressor gene (23). Several types of childhood tumor display a specific loss of the maternal 11p15 allele that suggests the involvement of an imprinted gene in this region (25).

BWS patients generally present with three major features: exomphalos, macroglossia and giantism. Other features include hypoglycemia, organomegaly, hemihypertrophy, genitourinary abnormalities, cleft palate and a susceptibility to embryonal tumors. In turn, TNDM is associated with intrauterine growth failure, dehydration, hyperglycemia and failure to thrive (26,27). There have been a number of reported associations with TNDM including umbilical hernia (7%) and macroglossia (23%) (28). These two anomalies are also found in patients with BWS, which typically also involves hyperinsulinemia. The role for *ZAC* is a predicted gain of function with biallelic expression of *ZAC* in TNDM patients (since UPD of the region also results in TNDM). Loss of function of $p57^{KIP2}$ in BWS is implicated in patients with point mutations within the coding sequence of the gene (29–32).

Several imprinted genes lie within the 11p15.5 region. *LIT1* (*KCNQ1OT1*), hereafter referred to as *LIT1*, is a paternally expressed, antisense RNA located within the *KCNQ1* gene that may regulate imprinting of the 11p15.5 domain (25). Differential methylation of the *LIT1* CpG island is conserved between human and mouse (25). This differential methylation is acquired in the germ line (33) making it an excellent candidate for an ICR. Frequent loss of maternal methylation at the *LIT1* CpG island has been observed in BWS patients (40–50%) (34). A targeted deletion of *LIT1* leads to loss of silencing of $p57^{Kip2}$ in both mice and in human cell lines (33,35). Finally, the region between the *Kcnq1* and $p57^{Kip2}$ shows both physical and mechanistic similarities to the imprinted domain containing *Igf2r* and its antisense control transcript, *Air* (36).

We, therefore, investigated whether the similarity in phenotypes between BWS and TNDM is a reflection of a regulatory association between *ZAC* and $p57^{KIP2}$.

MATERIALS AND METHODS

Cell lines

Human ovarian cancer (HOC) cell lines (PA-1 and SKOV-3) were used in this study. The source of these cells is as described previously (37). They were grown in either DMEM or RPMI1640 supplemented with 10% fetal bovine serum.

Bisulfite PCR methylation assay

Genomic DNAs from primary leucocytes from 17 TNDM patients, 8 BWS patients and 2 normal individuals were prepared as described previously (20). DNA (0.3μg) was digested with EcoRI. Bisulfite treatment was carried using the EZ DNA methylation kit (Zymo research) according to the manufacturer's instructions. PCR was carried out using the following primers. Primes sequences for the PCR: For *ZAC*: BS2F (ZAC), 5′-GTTTTTTATGTGTGATTGGGTTTTGGYGG-3′ and BS2R (ZAC), 5′-AAAACRCTAAAACCCCTAACRAAAAC-3′. For *LIT1*: BS2F (LIT1), 5′-TAGGATTTTGTTGAGGAGTTTTTTGG-3′ and BS2R (LIT1), 5′-CCACCTCACACCCAACCAATACCTCACATAC-3′. PCR condition was as follows: denaturation at 95 C for 30 s, annealing at 57 C for 30 s and extension at 72 C for 30 s for 30 cycles. PCR products were digested with the appropriate restriction enzyme (for *ZAC*: BssHII and RsaI; for *LIT1*: AciI and MaeIII) and electrophoresed on 2.5% agarose gels. PCR products were subcloned into the TA-TOPO cloning vector (Invitrogen) and sequenced.

Southern blotting

The methylation status of the *LIT1* CpG island was assessed by Southern blotting. Genomic DNAs were digested with BamHI alone or with the methylation sensitive enzyme NotI and electrophoresed on a 0.8% agarose gel, transferred onto Hybond-N^+ filter and fixed by UV cross-linking. The filter was hybridized with the *LIT1* CpG island 1.5 kb probe as described previously (25). Hybridization was carried out at 65 C overnight in Church-Gilbert buffer. Filters were washed with 0.1× SSC, 0.1% SDS at 65 C.

For the transient transfection assay, we examined the methylation status of the transfected plasmids by Southern blotting. Genomic DNAs from the transfected cultured cells (unmethylated and methylated plasmids) were prepared and digested with BamHI and XbaI with or without the methylation sensitive enzyme, HpaII. The plasmids were used as the hybridization probes. Blotting and washing were described as above.

In situ hybridization analysis

Mouse cDNA clones for *Zac1* and $p57^{Kip2}$ were used to prepare sense and antisense RNA by *in vitro* transcription using the DIG RNA labeling kit (Boehringer Mannheim). Sagittal and transverse sections of 8 μm from mouse embryos and placentas at E12.5 were used for *in situ* hybridization, essentially as described previously (38). Sections were counter stained with 4% eosin.

Band shift assay

Oligonucleotides were synthesized for the human $p57^{KIP2}$ CpG island including one putative ZAC binding site (accession number AC005950 and position of sequence 89690–89770) and for the *LIT1* CpG island including three putative ZAC binding sites (accession number U90095 and position of sequence 67890–67810). Where stated, the oligonucleotides were methylated with SssI methylase (New England Biolabs). Nuclear extracts were prepared from 293T cells transfected with the pAc5.1/V5-His, an expression vector (Invitrogen), according to the method of Schreiber *et al.* (39). For a band shift assay, the unmethylated or methylated double-strand DNA oligonucleotides (0.2 ng) were end-labeled with [γ-^{32}P]ATP and were incubated on ice for 30 min with the nuclear extract in 10 μl binding buffer [20 mM HEPES (pH 7.4), 1 mM EDTA, 3 mM $MgCl_2$, 60 mM KCl, 10 mM 2-mercaptoethanol, 4% glycerol, 0.1% Triton X-100 and 1 μg of poly(dI–dC)]. Excess (molar excess of 20-, 100- or 200-fold) unlabeled competitor oligonucleotides of the *LIT1* and $p57^{KIP2}$ CpG islands, either unmethylated or methylated, were added to the reaction mixture. The DNA–protein complexes were then electrophoresed on 5% acrylamide gels.

The super shift assay was performed by adding 0.2–1.0 μg ZAC antibody (Sigma) after 20 min of preincubation of nuclear extract with labeled unmethylated oligonucleotides of the human *LIT1* CpG island.

Methylation-dependent transcriptional repression assay

To test the effect of DNA methylation on the human *LIT1* CpG island we used a transient transfection assay in HeLa cells. A fragment containing the *LIT1* CpG island was generated by PCR using primers (F and R as shown in Figure 3) bearing specific restriction sites at their 5′ and 3′ ends. The primer sequences were as follows: F, 5′-ACTTGAAGGAAAGCAGGCAGGCAGGCAGGAT-3′; R, 5′-CCAACTGGAAGTTTGAGTGGAGTCCTGTTG-3′. PCR products were digested, gel-purified and subcloned into the pGL3-Promoter Firefly Luciferase reporter vector (Promega). Fragments LIT-W (869 bp NotI–HpaI), LIT-X (411 bp NotI–SacI), LIT-Y (458 bp SacI–HpaI) and LIT-Z (387 bp HpaI–R) were generated using the restriction sites present within the *LIT1* CpG island. Plasmids were prepared using a midi prep kit (Qiagen). *In vitro* DNA methylation was performed by incubation with CpG methylase. DNA constructs (2 μg) were transfected into HeLa cells, cultured for 22 h, lyzed and luciferase reading assayed. Firefly luciferase values were normalized against a co-transfected Renilla luciferase reporter, as described in the DLR assay protocol (Promega). Each construct was tested in triplicate in each experiment and the experiment was repeated three times.

Transactivation luciferase assay

The fragment used in the transcriptional activation assay was cloned into PicaGene Enhancer Vector 2 (NIPPON GENE). This fragment corresponds to LIT-X (411 bp) from within the *LIT1* CpG island. It was used unmethylated or *in vitro* methylated (LIT-X me). The human *ZAC* cDNA fragment was cloned into the pSG5 expression vector (Promega). DNA constructs were transfected into cultured cells with the reporter genes using Lipofectamine (Invitrogen). Samples were taken after 48 h, lyzed and luciferase readings taken. Firefly luciferase values were normalized against the control luciferase reporter vector.

RESULTS

Comparison of the expression pattern of the mouse *Zac1* and $p57^{Kip2}$ genes

Zac1 and $p57^{Kip2}$ appear to be expressed in many of the same tissues (7,20,40,41). Given the precedent for co-ordinated regulation of imprinted genes (4), we decided to investigate this more rigorously. We first compared the expression patterns of *Zac1* and $p57^{Kip2}$ in adjacent sagittal sections of E12.5 (embryonic day 12.5) mouse embryos. The genes showed a strikingly similar expression pattern in many tissues. There was strong expression in the lung, tongue, sclerotome, telencephalon and the labyrinth layer of the placenta (Figure 1A, B and D). Both genes were also expressed in Rathke's pouch (Figure 1D), the lumen of cardiac ventricle and bronchus of the lung (Figure 1E) and the epithelium of the adult ovary (Figure 1F). This is the developmental origin of ovarian cancers. We detected some differences in the pattern of expression of the two genes. $p57^{Kip2}$ was detected in the neural epithelium (Figure 1G), the equatorial region of the lens (Figure 1H) and retina (Figure 1I), the nasal epithelium (Figure 1J) and mesonephrum (Figure 1K) where expression of *Zac1* was absent.

The ZAC protein binds within the *LIT1* CpG island

The striking similarity in expression between mouse *Zac1* and $p57^{Kip2}$ raises the possibility of an interaction between two genes. The presence of a zinc finger motif within the ZAC protein suggests a DNA-binding capability. The consensus binding sequence for the ZAC protein has been identified as GGGGCCTC (17). We found that the CpG island of the human $p57^{KIP2}$ gene contains two ZAC binding sites (Figure 2A and B). Given the proposed role for the *LIT1* transcript in regulating the expression of $p57^{KIP2}$, we also looked for ZAC binding sites within the *LIT1* CpG island and found eight potential binding sites (Figure 2A and B).

We used an electromobility gel shift assay to ask whether the human ZAC protein could bind either of these regions.

Cell extracts containing the ZAC protein were incubated with the *LIT1* and $p57^{KIP2}$ CpG island oligonucleotides containing the putative ZAC binding sites. The probes were either unmethylated (M) or methylated (M+). A band shift analysis was performed (Figure 2C). The ZAC protein bound preferentially to unmethylated, a portion of the *LIT1* CpG island probe that contained the putative ZAC binding sites. No detectable binding was observed to the $p57^{KIP2}$ CpG island probe (data not shown). The binding was specific as only the unlabeled, unmethylated *LIT1* CpG island probe competed out the binding and not the $p57^{KIP2}$ CpG island probe or the methylated *LIT1* CpG island probe. Furthermore, specificity of this DNA–protein complex was confirmed in a super shift assay using an anti-ZAC antibody (Figure 2D). This suggests that ZAC protein may bind to the *LIT1* CpG island *in vivo* and perhaps indirectly regulate $p57^{KIP2}$ expression.

Methylation-dependent transcriptional repression assay of the *LIT1* CpG island

There is evidence to suggest that the *LIT1* transcript may regulate imprinting of the 11p15.5 domain. This differentially methylated *LIT1* CpG island is conserved between human and mouse (25). The differential methylation is acquired in the germ line (33) making it an excellent candidate for an ICR.

To determine whether the *LIT1* differentially methylated region has the capacity to function as a regulatory element, we tested it in a transient transfection assay in HeLa cells in which a reporter gene (firefly luciferase) was expressed from an SV40 promoter. Unmethylated or methylated fragments from the human *LIT1* CpG island were assayed for their effect

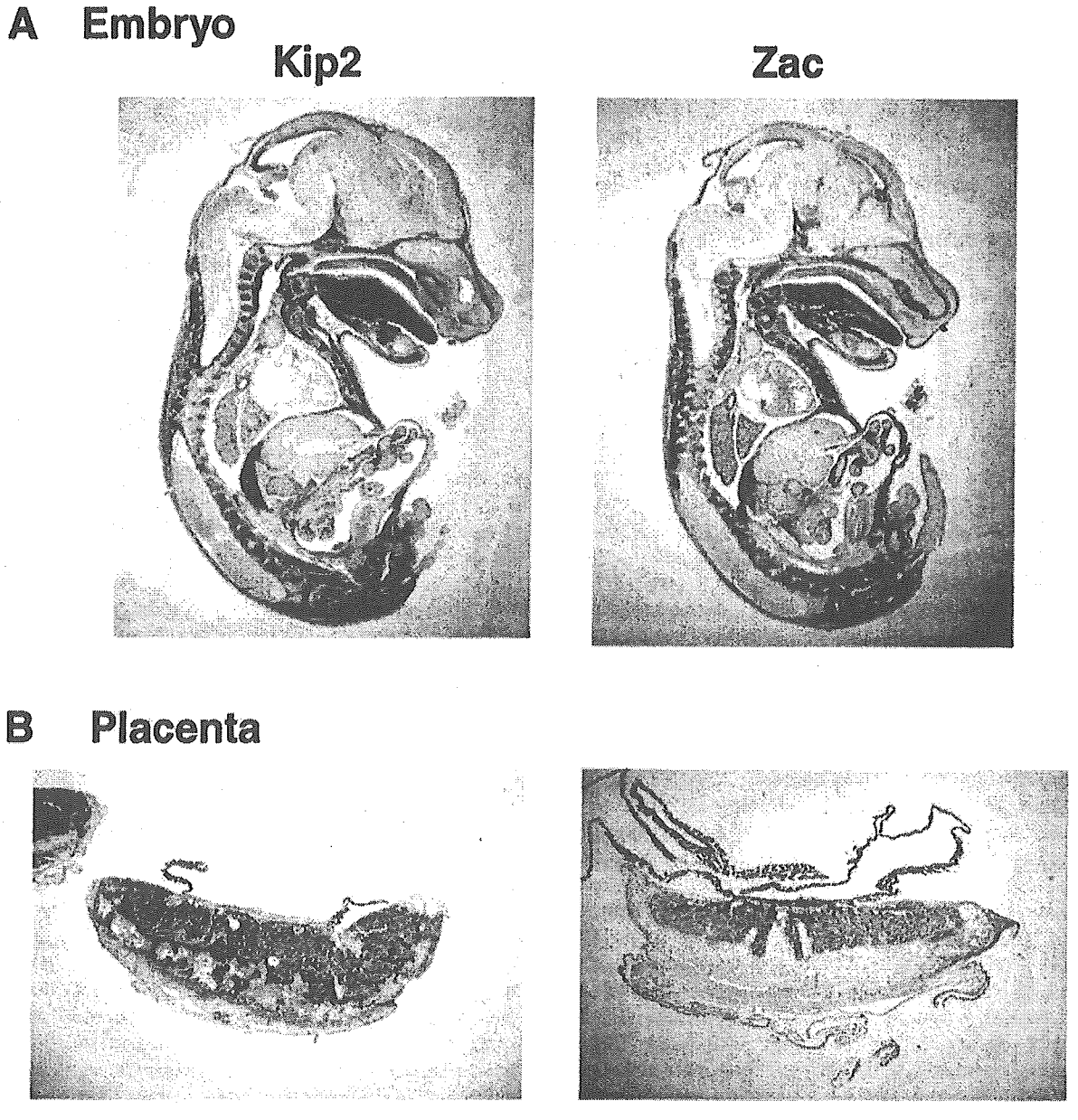

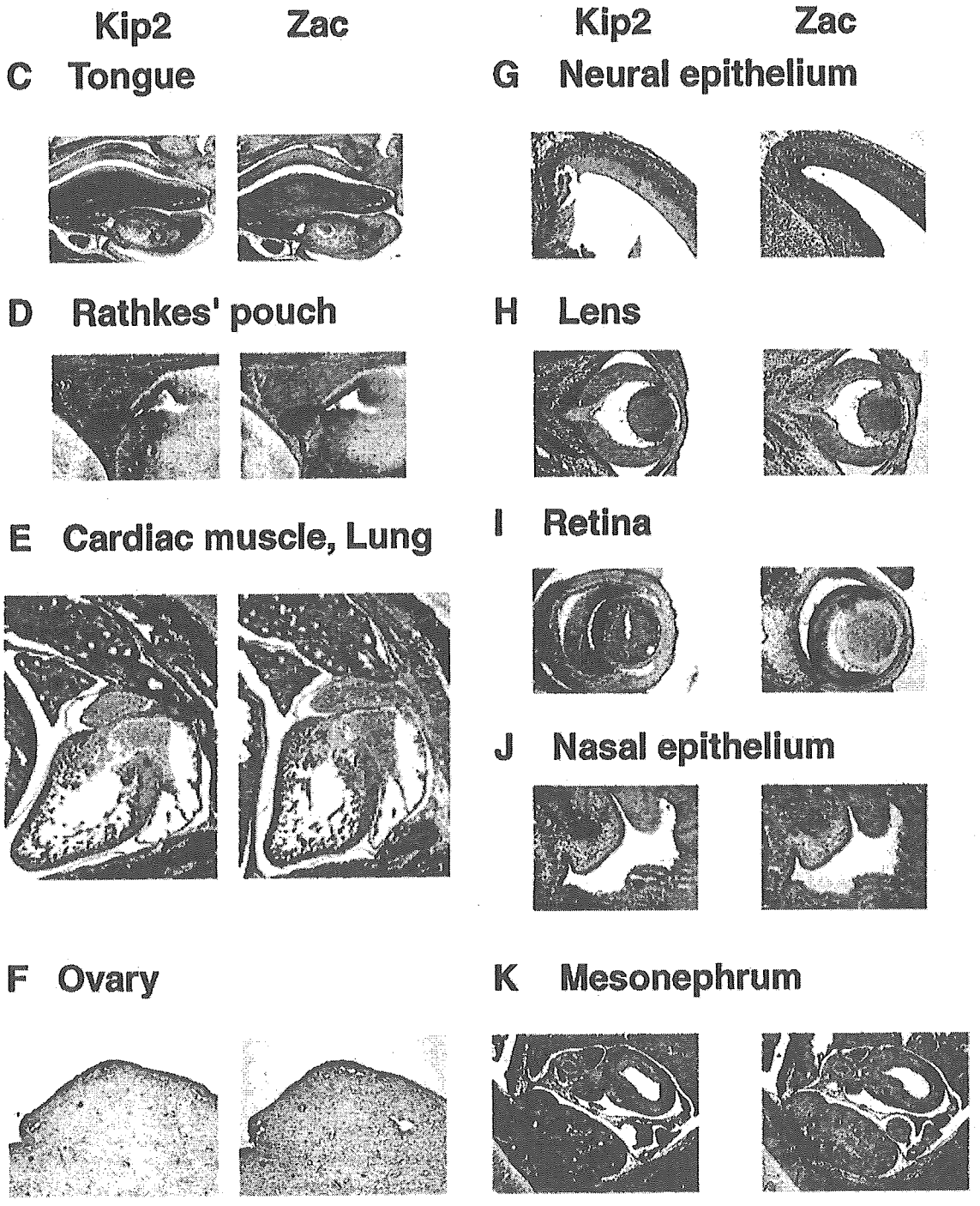

Figure 1. Expression of *Zac1* and $p57^{Kip2}$ in mouse embryos and adult ovary. The comparison of the tissue-specific expression in adjacent sagittal sections of E12.5 embryos (**A**) and placenta (**B**) by *in situ* hybridization. The two genes show striking similarities in their expression patterns. (**C–K**) Detailed analysis of expression during embryonic development of *Zac1* and $p57^{Kip2}$ in transverse and/or sagittal sections of E12.5 embryo. Tongue (C), Rathke's pouch (D), heart and lung (E), telencephalon (G), lens (H), retina (I), nose (J) and mesonephrum (K). Expression of the genes was examined in adult ovary (F).

on transcription of the reporter (Figure 3A). The maintenance of their methylation status after transfection was confirmed by Southern blotting (Figure 3B). Among the fragments we tested, the LIT-X (411 bp NotI–SacI), which contains 57 CpG sites, was shown to act as a strong transcriptional silencer, but only when methylated (Figure 3A). Significantly, the cluster of the ZAC binding sites is present within this region. In contrast, methylation of the LIT-Y fragment, which contains 55 CpG sites, caused negligible repression of the reporter gene (Figure 3A). Interestingly, the LIT-X fragment is contained within a larger fragment (LIT-W) which has a lower repression activity. This may be due to the inclusion of the *LIT1* promoter within the larger LIT-W fragment (M. Oshimura, unpublished data). This promoter may harbor both transcriptional activation and repression properties in this assay. This indicated that LIT-X within the ICR can function

as a *cis*-regulatory element and capable of strong transcriptional silencing in this assay.

Although a large CpG island is present in the 10th intron of *KvLQT1* in both human and mice, its primary sequence is poorly conserved. However, in mice the region containing the DNase I hypersensitive sites within the *Lit1* CpG island, which are upstream of the transcription initiation site, is critical for promoter activity (42,43). The transcriptional initiation site of human *LIT1* gene has been determined in an RNase protection assay and by primer extension analysis by M. Oshimura *et al.* (personal communication). The transcription initiation site is at 67499 nt (U90095) and lies within the *LIT1* CpG island. Also present are two putative CCAAT boxes and a Sp1-binding site but no TATA-box. There is also an AP-1 site downstream of this region. The distal region including F-SacI fragment was previously reported to act as a silencer (44). In mouse, a fragment containing both the hypersensitive sites and the transcriptional start site displayed the strong silencing activity (42). According to the model proposed by Constancia *et al.* (45) repeat sequences may play a role in the methylation of CpG islands. It is interesting that this distal region also contains two direct repeats.

Cell transfection assay

We established an assay to examine whether ZAC binding activates transcription from the *LIT1* promoter. We used two ovarian cancer cell lines (PA1 and SKOV) in which we had shown that endogenous *ZAC* expression was absent (46). These lines were transfected with a luciferase reporter vector with the LIT-X fragment. We also transiently transfected a *ZAC* expression construct into these cells and then measured luciferase activity. *ZAC* behaved as a transcriptional activator (Figure 4) consistent with our binding assay results. Furthermore, when we assayed whether the ZAC protein would activate the methylated *LIT1* reporter in the SKOV ovarian cancer cell line, we did not observe any activation of the reporter suggesting that *ZAC* acts in a signaling pathway only on the unmethylated, paternal *LIT1* allele *in vivo*.

Epigenetic changes at the *ZAC* ICR in BWS and the *LIT1* ICR in TNDM patients

The similarity in phenotypes between BWS and TNDM may reflect a regulatory association between *ZAC* and $p57^{KIP2}$. Our data suggest a possible pathway where over expression of *ZAC*, possibly by loss of methylation of the *ZAC* CpG island, may hyperactivate the *LIT1* gene and silence $p57^{KIP2}$. We therefore examined the imprinting status of *ZAC* in BWS patients and *LIT1* in TNDM patients.

We examined the methylation status of the *ZAC* and *LIT1* DMRs in both types of patients. We performed the restriction enzyme digest and sequencing after PCR of bisulfite-modified genomic DNA (47). After bisulfite treatment of genomic DNA from 8 BWS and 17 TNDM patients, PCR products were digested with AciI and MseIII for the *LIT1* CpG island and RsaI and BssHII for the *ZAC* CpG island (Figure 5A). In this assay, a methylated cytosine will maintain the enzyme recognition site and will be cut, whereas the unmethylated cytocine is converted to thymidine destroying the recognition site. In addition, sodium bisulfite-treated DNA was PCR amplified, subcloned, sequenced and the methylation status was determined at 22 CpG sites in the *ZAC* locus and at 24 CpG sites within the *LIT1* locus. All 8 BWS patients showed normal methylation patterns in *ZAC* (Figure 5B) but 2 TNDM patients

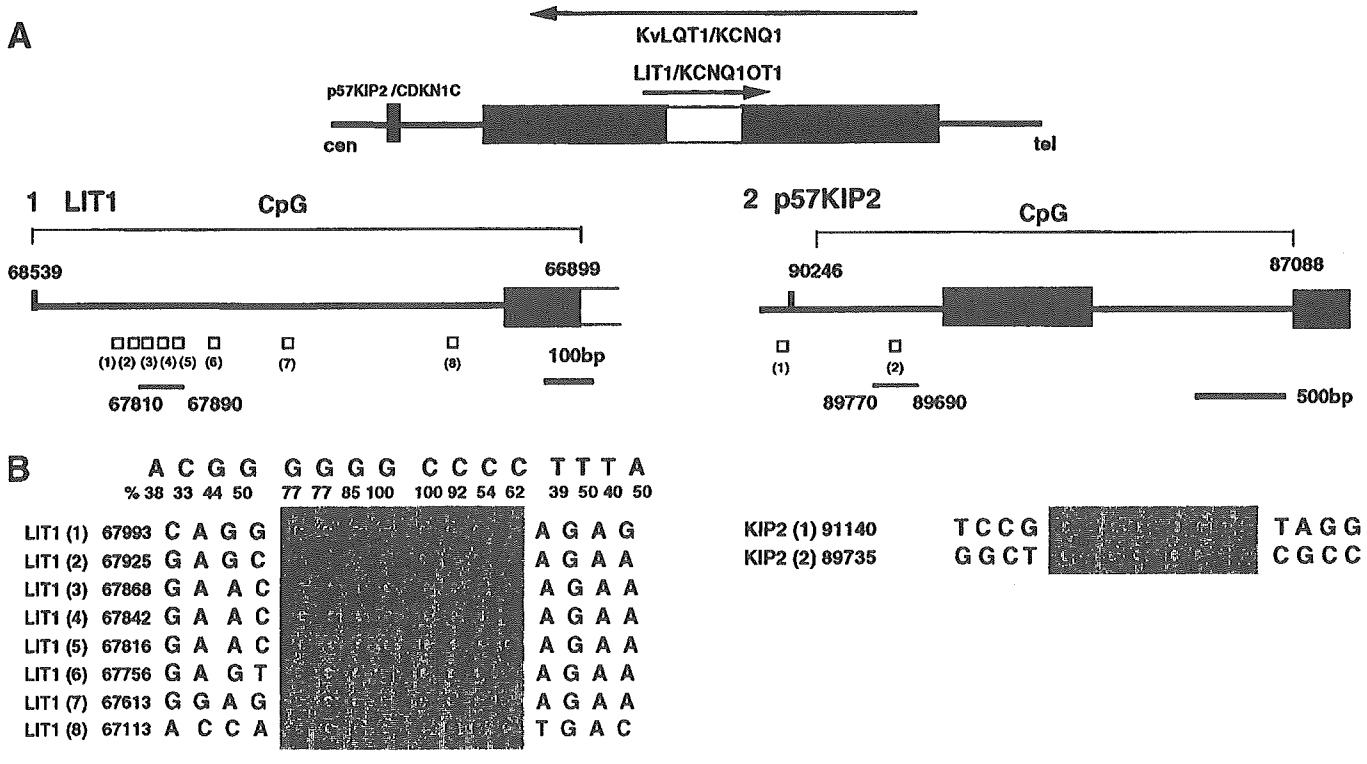

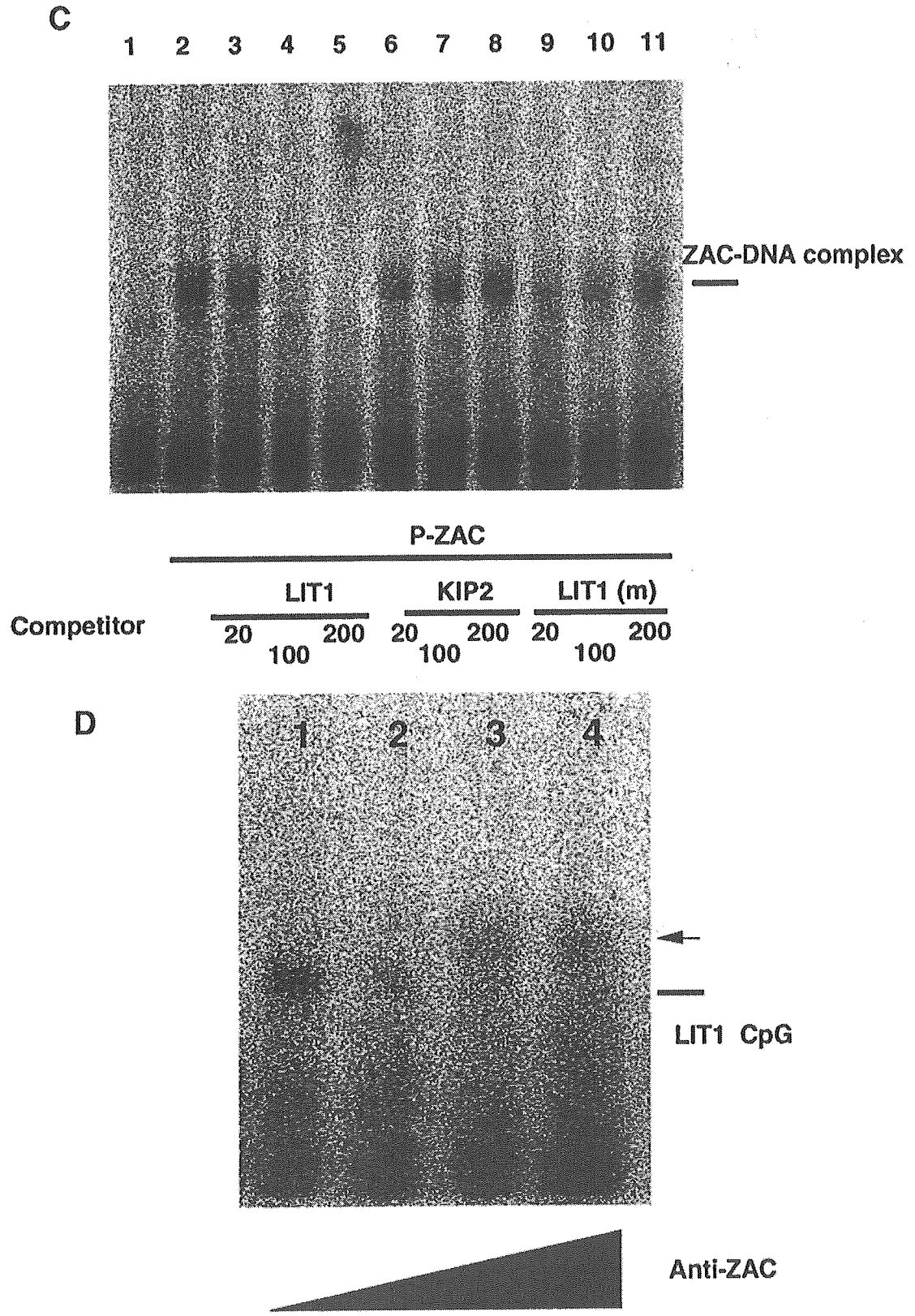

Figure 2. ZAC binds to the *LIT1* CpG island. (**A**) Map of the ZAC binding sites clustered in the *LIT1* CpG island and the two sites in the $p57^{KIP2}$ CpG island. Open boxes indicate putative ZAC binding sites. (**B**) Sequences of the ZAC binding sites within *LIT1* and $p57^{KIP2}$ CpG island. (**C**) Band shift of DNA complexed with ZAC protein. [γ-^{32}P]ATP-labeled oligonucleotides containing CpG islands from *LIT1* were incubated without recombinant ZAC protein (lane 1) and with an ZAC protein (lanes 2–11). The *in vitro* methylation of CpG sequences (me) was performed with SssI methylase. Various cold (unlabeled) competitors of *LIT1*, *KIP2* and *LIT1*(me) oligonucleotides were used in excess: 20-fold molar excess (lanes 3, 6 and 9), 100-fold (lanes 4, 7 and 10) and 200-fold (lanes 5, 8 and 11). (**D**) Specificity of the ZAC protein–*LIT1* CpG island probe complex was confirmed in a super shift assay using an antibody to ZAC; 0 µg (lane 1), 0.2 µg (lane 2), 0.5 µg (lane 3) and 1.0 µg (lane 4).

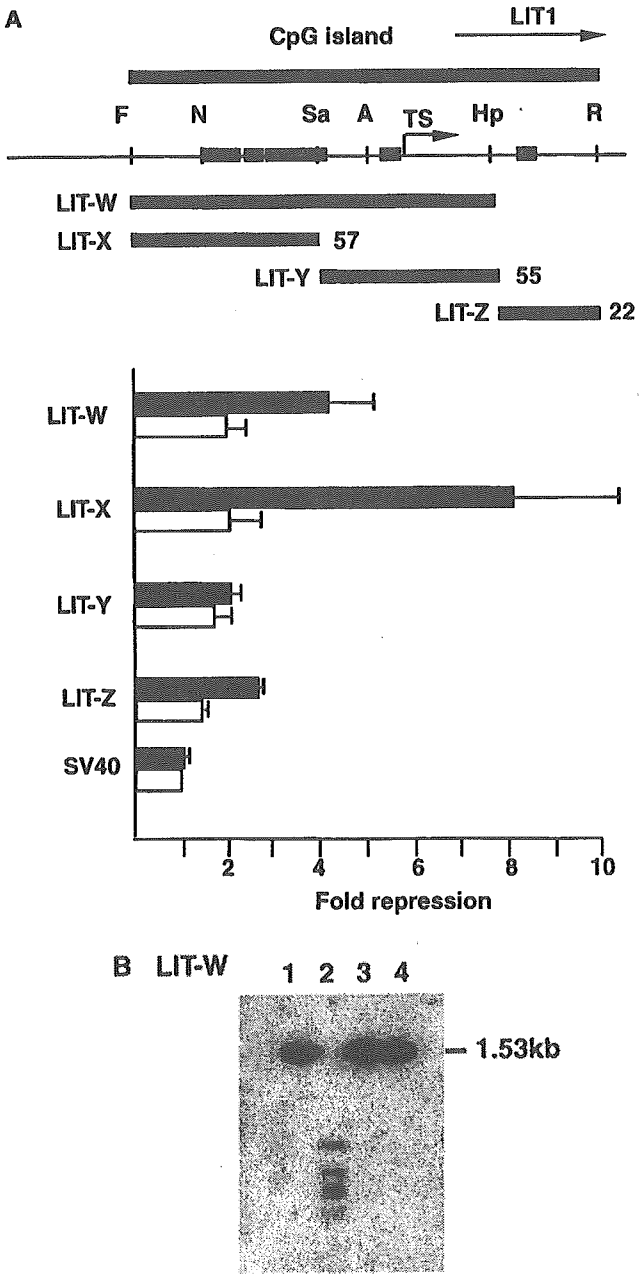

Figure 3. Methylation-dependent transcriptional repression by the *LIT1* CpG island. (**A**) The map indicates the regions of human *LIT1* CpG island tested in the transfection assay. The number of CpG dinucleotides present in each fragment is indicated. The light emission obtained from the SV40 promoter alone, either unmethylated (open bars) or after methylation with SssI methylase (closed bars) was normalized to a value of one and the fold repression of *LIT1* CpG island-containing constructs was calculated relative to these values, shown in the graph. All firefly luciferase values were normalized against a co-transfected Renilla luciferase reporter driven by a thymidine kinase (TK-Renilla) promoter. Cells transfected with TK-Renilla alone demonstrated no firefly luciferase activity. Error bars show calculated SEM values for repeated experiments. Gray boxes show the putative binding sites for ZAC. F and R show the locations of the primers to amplify the CpG island, Sa is SacI site; A is AscI site; N is NotI site; Hp is HpaI site. TS is transcriptional start site (M. Oshimura, unpublished data). (**B**) Maintenance of the methylation status after transfection. Genomic DNAs from cells transfected with either unmethylated or methylated plasmid DNA were examined by Southern blotting. DNAs from unmethylated LIT-W transfected cells (lanes 1 and 2) and SssI-methylated LIT-W (lanes 3 and 4) were digested with BamHI and XbaI without (lanes 1 and 3) and with the methylation sensitive restriction enzyme HpaII (lanes 2 and 4).

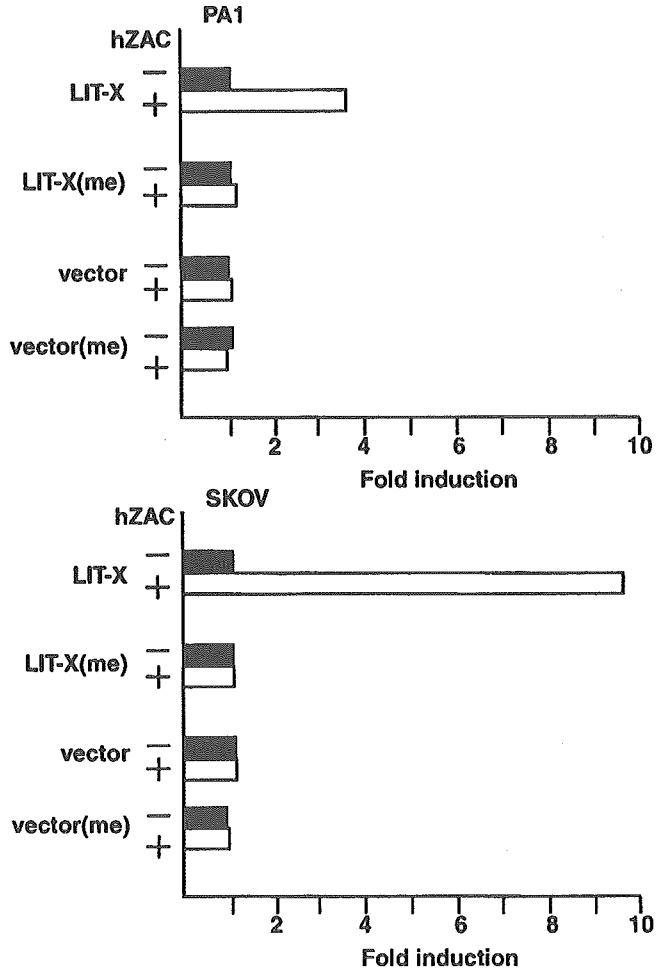

Figure 4. Transcriptional activation of the *LIT1* CpG island by ZAC. Two HOC cells (PA1 and SKOV) were transiently co-transfected either with the unmethylated (LIT-X) or with the methylated [LIT-X(me)] reporter genes without the SV40 promoter in combination with the *ZAC*-pSG5 expression vector. pSG5 vector DNA without the *ZAC* cDNA insertion was used as a control.

showed loss of methylation in the *LIT1* CpG locus (Figure 5B, data shown for AciI). One of these patients exhibited UPD of chromosome 6 (UPD6). The other patient had a normal karyotype and loss of methylation on the maternal *ZAC* DMR region. Sequencing revealed that all 24 *LIT1* CpG sites were predominantly unmethylated in both patients (Figure 5C). The second patient was characterized with TNDM complicated with umbilical hernia and macroglossia, features commonly seen in BWS patients. Finally, we confirmed loss of methylation at the *LIT1* locus in these two patients by a second technique, Southern blotting. (Figure 5D). Both patients showed loss of differential methylation of the *LIT1* locus in association with presumed biallelic expression of *ZAC*.

DISCUSSION

While investigating the function of *ZAC*, an imprinted tumor suppressor gene, we found that this gene has a strikingly similar expression pattern to a second imprinted gene, $p57^{Kip2}$. In humans, *ZAC* is a candidate in TNDM while

$p57^{KIP2}$ has been shown to play a role in BWS. In addition to the similarity in expression, we noticed that some of the features seen in BWS, such as tumors, intrauterine growth abnormalities, umbilical hernias, macroglossia and defects in insulin are also found in TNDM patients metabolism.

We were unable to demonstrate a direct interaction between the ZAC transcription factor and the $p57^{KIP2}$ gene. However, we found that ZAC bound to, and activated expression of a third imprinted gene, *LIT1*. *LIT1* has been shown to act an ICR that negatively regulates the $p57^{KIP2}$ gene in *cis*. Though few BWS patients have genetic mutations in the $p57^{KIP2}$ gene itself, nearly 60% showed loss of methylation of the *LIT1* CpG island. By showing that *ZAC* directly binds to the *LIT1* CpG island *in vitro* and activates transcription, we have identified a possible role for ZAC in the regulation of $p57^{KIP2}$.

We have shown that some patients with TNDM (2 out of 17) have defects in methylation of *LIT1* CpG island, supporting a link between these genes. Furthermore, ZAC has similarities with p53, a known tumor suppressor gene. p53 regulates p21, a member of the same family of cyclin-dependent kinase inhibitors as $p57^{KIP2}$. Since our data suggest that *ZAC* may regulate $p57^{KIP2}$, the two genes may form part of a signaling pathway for regulating cell cycle progression. p73, a homologue of p53, was suggested as an imprinted gene (48) and more recently has been shown to directly regulate $p57^{KIP2}$ (49). Further work is required to link these genes but our initial conclusion is that we have potentially identified a novel imprinted pathway similar to the *Igf2/Igf2r* pathway.

Finally, our finding that *ZAC* may indirectly regulate $p57^{KIP2}$ indicates a potential role for *ZAC* in BWS. While we did not detect changes in DNA methylation at the *ZAC* CpG island in BWS patients, we were only able to survey a small number of patients. We did find changes in *LIT1* DNA methylation in two TNDM patients suggesting a more global defect in imprinted DNA methylation in these patients.